CD4+CD57+ Senescent T cells as Promoters of Systemic Lupus Erythematosus Pathogenesis and the Therapeutic Potential of Senolytic BCL-2 Inhibitor

Journal:	*European Journal of Immunology - 2*
Manuscript ID	eji.202350603.R1
Wiley - Manuscript type:	Research Article
Date Submitted by the Author:	08-Feb-2024
Complete List of Authors:	Jiang, Jiao Yang, Ming Zhu, Huan; Central South University, Long, Di; Second Xiangya Hospital Department of Dermatology, He, Zhenghao; The Second Xiangya Hospital of Central South University, Dermatology Liu, Juan He, Liting Tan, Yixin; Second Xiangya Hospital Department of Dermatology, Department of Dermatology Akbar, Arne N.; UCL, Reddy, Venkat Zhao, Ming Long, Hai Wu, Haijing Lu, Qianjin
Keywords:	Aging, Autoimmunity, CD4 T cells, Clinical immunology, Skin diseases/ immunology
Keywords:	Systemic Lupus Erythematosus, CD4+ T cell, Cellular senescence, CD57, senolytics

Full title: $CD4^+CD57^+$ Senescent T cells as Promoters of Systemic Lupus Erythematosus~~SLE~~ Pathogenesis and the Therapeutic Potential of Senolytic BCL-2 I~~i~~nhibitor~~ in Ameliorating Mouse Model of SLE~~~~IL-15-mediated $CD4^+$ T Cell Senescence Promotes the Development of Systemic Lupus Erythematosus~~

Running title: Senescent T cells promote SLE and BCL-2 inhibitor as a therapeutic potential

Authors: Jiao Jiang[1, 2], Ming Yang[2], Huan Zhu[2], Di Long[2], Zhenghao He[2], Juan Liu[2], Liting He[2], Yixin Tan[2], Arne N. Akbar[3], Venkat Reddy[3], Ming Zhao[1, 2], Hai Long[#2], Haijing Wu[#2], and Qianjin Lu[#1, 2]

Affiliations:

[1] Hospital for Skin Diseases, Institute of Dermatology, Chinese Academy of Medical Sciences & Peking Union Medical College~~Institute of Dermatology, Chinese Academy of Medical Sciences and Peking Union Medical College~~, Nanjing, Jiangsu, China.

[2] Department of Dermatology, Hunan Key Laboratory of Medical Epigenomics, The Second Xiangya Hospital of Central South University, Changsha, Hunan, China.

[3] Division of Medicine, University College London, London, WC1E 6JF, United Kingdom.

[4] Centre for Rheumatology, Division of Medicine, University College London, London, WC1E 6JF, United Kingdom.

Address correspondence to Hai Long, The Second Xiangya Hospital of Central South University, 139 Renmin Middle Road, Changsha, Hunan 410011, P.R.China. Phone and fax number: +86-731-85294099; Email: dr.hailong@csu.edu.cn. Or to: Haijing Wu, The Second Xiangya Hospital of Central South University, 139 Renmin Middle Road, Changsha, Hunan 410011, P.R.China. Phone and fax number: +86-731-85294099; Email: chriswu1010@csu.edu.cn. Or to: Qianjin Lu, Institute of Dermatology, Chinese Academy of Medical Sciences and Peking Union Medical College, #12 Jiangwangmiao Street, Nanjing, Jiangsu 210042, P.R.China. Phone and fax number: +86-731-85294099; Email: qianlu5860@pumcderm.cams.cn.

Keywords: Systemic Lupus Erythematosus, $CD4^+$ T cell, Cellular senescence, CD57, senolytics

Abbreviations list:

SLE, Systemic lupus erythematosus

SLEDAI, SLE Disease Activity Index Score

RA, Rheumatoid Arthritis

HCs, Healthy controls

ISGs, Interferon-induced genes

BCL-2, B-lymphoma-2

ABCs, Age-related B cells

ANA, Antinuclear antibody

SASPs, Senescence-associated secretory phenotypes

MMPs, Matrix metalloproteinases

GC, Germination center

MFI, Mean fluorescence intensity

Funding: This work was supported by the National Natural Science Foundation of China (No. 82273540, No.81830097, No.81972943, No.82173425, No.81773332), National Science and Technology Major Project (2020ZX09201-28), Hunan Talent Young Investigator (No. 2019RS2012), and Hunan Outstanding Young Investigator (No. 2020JJ2055), CAMS Innovation Fund for Medical Sciences (CIFMS)(2019-2M-5-033), National Key R&D Program of China (No.2021YFC2702004), and Central South University Innovation-Driven Research Programme (2023CXOD046). Dr. Venkat Reddy was supported by MRC-Clinical Academic Research Partnership Award (MR/T024968/1).

Conflicts of interest: The authors have no relevant financial or non-financial interests to disclose.

Author contributions: QL, HW, and HL designed the experiments. JJ and MY performed the experiments. JJ, MY, HZ, DL, ZH and JL analyzed data and performed statistical analyses. JJ drafted and edited the figures, and wrote the manuscript. All authors revised and approved the manuscript for publication.

Data availability statement: The data that support the findings of this study are available from the corresponding authors upon reasonable request.

~~IL-15-mediated Accumulation of Senescent $CD4^+$ T Cells Promotes the Development of Systemic Lupus Erythematosus~~

Abstract

Systemic lupus erythematosus (SLE) is an autoimmune disease characterized by persistent activation of immune cells and overproduction of autoantibodies. Senescent T and B cells accumulate in immune-mediated chronic inflammatory disease such as SLE. However, in SLE, the precise mechanistic pathways are not fully understood. We found that in SLE patients: 1) the frequency of $CD4^+CD57^+$ senescent T cells was significantly elevated and positively correlated with disease activity; 2) the expression levels of B-lymphoma-2 (BCL-2) family and interferon-induced genes (ISGs) were significantly upregulated; and 3) in vitro, incubation of isolated T cells with IL-15 increased the frequency of senescent $CD4^+$ T cells and upregulated the expression of BCL-2 family and ISGs. Further, treatment of MRL/lpr mice with ABT-263, a senolytic BCL-2 inhibitor, resulted in lower: 1) frequency of $CD4^+CD44^{hi}CD62L^-PD\text{-}1^+CD153^+$ senescent $CD4^+$ T cells; 2) the frequency of $CD19^+CD11c^+$T-bet$^+$ age-related B cells (ABCs); 3) levels of serum antinuclear antibody (ANA); 4) proteinuria; 5) frequency of Tfh cells; and 6) renal histopathological features. Collectively, these results indic~~i~~ated a dominant role for $CD4^+CD57^+$ senescent $CD4^+$ T cells in the pathogenesis of SLE and ~~mediated through IL-15-CD57-BCL-2/ISGs signaling pathway~~senolytic BCL-2 inhibitor ABT-263 may be the potential treatment in ameliorating SLE mouse model. ~~Thus, our study provides a mechanistic basis for targeting BCL-2 pathway as a~~

novel therapeutic strategy for SLE.

Keywords: Systemic Lupus Erythematosus, $CD4^+$ T cell, Cellular senescence, CD57, senolytics

Introduction

Systemic lupus erythematosus (SLE) is an autoimmune disease characterized by abnormal activation of immune cells and overproduction of autoantibodies, causing photosensitive skin rash, nephritis, oral ulceration, and arthritis[1]. SLE has a profound negative impact on the quality of life owing to significant morbidity and mortality. The etiology and pathogenesis of SLE are unclear and considered to be multifactorial including genetic susceptibility, and environmental factors such as ultraviolet rays, drugs, smoking, and infection can cause immune dysfunction through epigenetic mechanisms, ultimately leading to excessive autoantibodies and cytokines[1-4]. In this context, abnormal activation and differentiation of $CD4^+$ T cells play a key role in the pathogenesis of SLE[1, 5]. Current therapies for the majority of patients with SLE include a combination of immunomodulatory agent (hydroxychloroquine), immunosuppressants and glucocorticoids, which deliver moderate beneficial effects, but significant adverse effects[1]. Therefore, it is of critical importance to probe novel immunopathomechanisms toward developing novel therapies for SLE.

Recent evidence suggests that immune cell senescence as an important mechanism that contributes to chronic inflammation. Cellular senescence is a state of permanent cell cycle arrest that is triggered by internal and exogenous stimuli such as persistent cellular activation through antigen-dependent and cytokine mediated ‘bystander’ activation, chemotherapy drugs, radiation stress, high-fat diet, proto-oncogene activation, oxidative stress, mitochondrial dysfunction, and DNA damage[6]. Consequent

108 upregulated expression of cyclin-dependent kinase inhibitor 2A (CDKN2A) (encoding p16 protein) and CDKN1A (encoding p21 protein) in senescent cells, results in continuous activation of downstream p53 protein and irreversible cell cycle arrest[6] and p16 expression is considered to be an important marker of cellular senescence[7]. An intriguing feature of senescent cells is a high expression of the anti-apoptotic B-lymphoma-2 (BCL-2) family such as BCL-2 and BCL-xL[8] which confer relative resistance to apoptosis. In addition, senescent cells have a senescence-associated secretory phenotypes (SASPs) with potent secretion of proinflammatory cytokines, chemokines, growth factors, and extracellular matrix metalloproteinases (MMPs)[6, 8-13]. For example, proinflammatory cytokines such as IL-6, IL-8 and TNF alpha are important components of SASP[9]. Thus, in the long-term, senescent cells can accumulate to promote chronic inflammation leading to the development of age-associated multimorbidities such as cardiovascular diseases, neurodegenerative diseases and metabolism-related diseases, a phenomenon referred to as 'inflammaging' [6, 11-13].

Cellular senescence of many immune cell types, T cells and B cells in particular, contribute to inflammaging. A combination of surface markers, such as increased expression of CD57, KLRG-1, and the loss of costimulatory receptors CD27/CD28 help define senescent T cells [14, 15]. For example, $CD4^{+}CD44^{hi}CD62L^{-}PD\text{-}1^{+}CD153^{+}$ T cells (senescent $CD4^{+}$ T cells that found in mouse models) expressed cellular senescence-related markers p16 and p21 and had the effect of promoting inflammatory states and immune disorders[16]. $CD4^{+}CD57^{+}$ senescent T cells are significantly increased in the peripheral blood of patients with active Rheumatoid Arthritis (RA)[17-19]. An elevated level of CD4$^+$CD44^{hi}CD62L$^-$PD-1$^+$CD153$^+$ senescent CD4$^+$ T cells has been detected in the germination center (GC) of the (NZB × NZW) F1 lupus model suggesting their contribution to the pathogenesis of lupus erythematosus through promoting the production of autoantibodies such as ANA[20, 21]. Age-associated B cells (ABCs) also contribute to the pathogenesis of SLE. However, the role and underlying mechanism of senescent CD4$^+$ T cells and ABCs in the development of SLE remains unclear.

Here, we revealed that the CD4$^+$CD57$^+$ senescent T cells as promotersIL-15-CD57-BCL-2/ISGs signaling pathway was dysregulated in lupus pathogenesis and the senolytic BCL-2 inhibitor ABT-263, which provides a potential therapeutic strategy for SLE.

Results

1. The frequency of CD4$^+$CD57$^+$ senescent CD4$^+$ T cells in SLE patients was significantly elevated and positively correlated with disease activity.

We used flow cytometry to detect the frequency of senescent CD4$^+$CD57$^+$ T cells in peripheral blood of patients with SLE, RA, and healthy controls (HCs). WE found that the frequency of CD4$^+$CD57$^+$ senescent CD4$^+$ T cells of SLE patients was significantly increased (Figure 1A and B) and positively correlated with the SLE Disease Activity

Index (SLEDAI) Score (Figure 1C). Further, the mean fluorescence intensity (MFI) of CD57 in $CD4^+$ T cells of SLE patients was also significantly increased (Figure S1C) and positively correlated with the SLEDAI score (Figure S1D).

We grouped distinct SLE patients by disease activity, skin lesions, lupus nephritis, and autoantibodies, and compared the frequency of $CD4^+CD57^+$ senescent $CD4^+$ T cells between different subgroups of patients with SLE and HCs. We found that: 1) the proportion of senescent $CD4^+$ T cells in active SLE patients was significantly increased when compared with inactive SLE patients and HCs (Figure 1D); 2) the frequency of senescent $CD4^+$ T cells was significantly elevated in SLE patients with skin lesions when compared with SLE patients without skin lesions and HC (Figure 1D); 3) the proportion of senescent $CD4^+$ T cells increased in SLE patients with lupus nephritis and / or seropositivity for double-stranded DNA (dsDNA), anti-Smith (Sm), anti-RO52, or anti-U1-nRNP autoantibody relative to SLE patients with non-renal lupus or a negative result for corresponding autoantibodies (Figure 1D and S1F). Further, we found that the proportion of $CD4^+CD27^-CD28^-$ cells was significantly increased in peripheral blood of SLE patients (Figure S1A and B), however, there was no correlation with the SLEDAI score (Figure S1D). These results revealed significant relationship between the frequency of $CD4^+CD57^+$ senescent $CD4^+$ T cells in peripheral blood and seropositivity and clinical disease activity in SLE. Therefore, we focused on the role and underlying mechanisms of $CD4^+CD57^+$ senescent $CD4^+$ T cells in the pathogenesis of SLE.

Next, we focused on the role and underlying mechanism of $CD4^{+}CD57^{+}$ senescent $CD4^{+}$ T cells in the pathogenesis of SLE. We isolated $CD4^{+}$ T cells from peripheral blood of SLE patients and HCs, and used reverse transcription quantitative PCR (RT-qPCR) to detect mRNA expression levels of key senescence-related markers *CD57*, *p16*, *p21*, *p53*, and also critical SASP components including *IL6*, *IL8*, and *TNFα* in $CD4^{+}$ T cells.

We found that the mRNA expression levels of *CD57*, *p16*, *p21*, *p53*, *IL6*, *IL8*, and *TNFα* in the $CD4^{+}$ T cells of SLE patients were significantly higher than those in HCs (Figure 1E). Besides, the mRNA expression level of *CD57* was positively correlated with SLEDAI scores (Figure 1F), and partly correlated with ESR, C3, and C4 (Figure 1F). The mRNA expression level of *CD57* in peripheral $CD4^{+}$ T cells of SLE patients was positively correlated with the mRNA expression levels of cellular senescence-related markers *p16* and *p53* (Figure S1E).

Similarly, we grouped distinct SLE patients by skin lesions, lupus nephritis, and serum autoantibodies, and then compared the mRNA expression level of *CD57* between different SLE groups and HCs. We found that: 1) the mRNA expression level of *CD57* in SLE patients with a positive anti-U1-nRNP autoantibody was significantly higher than those in SLE patients with a negative anti-U1-nRNP autoantibody (Figure 1G); 2) the mRNA expression levels of *CD57* in SLE patients with skin lesions, with lupus nephritis, or with a positive anti-dsDNA, anti-Sm, anti-Nucleosome Antibody (ANuA), anti-ribosomal P autoantibodies (P), or anti-SSA were significantly higher than those in HCs, while slightly higher than those in SLE patients with a corresponding negative result (Figure S1G).

2. Increased frequency of $CD57^+$ senescent Tfh-like cells in SLE patients.

Next, we analyzed the proportion of senescent T cells in peripheral $CD4^+$ T cell subset of SLE using flow cytometry of PBMCs from patients with SLE, RA, and HCs according to the previously reported biomarkers[22-24] (Figure 2A and S2A). We found that the frequency of $CD57^+$ senescent Tfh-like cells in SLE patients was significantly higher than those in RA patients and HCs (Figure 2B). Further, in SLE patient samples, the proportion of $CD57^+$ senescent Tfh-like cells was also significantly greater than in the subpopulation of Treg, Th1, Th2, and Th17 cells (Figure 2D). Also, the frequency of $CD57^+$ senescent Th1 cells in SLE was significantly higher than those in HCs, while slightly higher than those in RA patients (Figure 2B) and significantly higher than $CD57^+$ senescent Treg, Th2, and Th17 cells in SLE (Figure 2D). The proportion of $CD57^+$ T cells in $CD4^+CD45RA^-$ T cells in SLE was significantly higher than those in RA patients and HCs (Figure 2C), while there was no difference in the frequency of $CD57^+$ T cells of $CD4^+CD45RA^+$ T cells among SLE patients, RA patients, and HCs (Figure 2C). Finally, the frequency of $CD27^-CD28^-$ cells in Tfh-like cells of SLE patients was also significantly higher than that of RA patients and HCs (Figure 2E).

We performed the human Tfh differentiation in peripheral naïve T cells and found that the mRNA expression of *p21* gradually increased during the Tfh differentiation (Figure

2F). The mRNA expressions of *p21* in differentiated Tfh cells were significantly higher than in naïve T cells (Figure 2F), and the mRNA expression of *p21* in differentiated Tfh cells (on day 5) was slightly higher than in differentiated Tfh cells (on day 3) (Figure 2F).

3. Increased expressions of BCL-2 and interferon-stimulated genes (ISGs) in senescent $CD4^+$ T cells of SLE.

We performed flow cytometry to detect the expression of BCL-2 in peripheral senescent $CD4^+$ T cells from patients with SLE (Figure 3A). The results showed that the MFI of BCL-2 in peripheral $CD4^+$ T cells of SLE patients was significantly higher than that of HC (Figure 3B and 3D). Similarly, the MFI of BCL-2 in $CD4^+CD57^+$ senescent $CD4^+$ T cells of SLE patients was also significantly higher than that of HC samples (Figure 3C and 3E).

Next, we performed RT-qPCR to detect mRNA expression levels of BCL-2 family members (*BCL2* and *BCLxL*) genes in peripheral $CD4^+$ T cells of SLE patients and HCs. The results showed that the mRNA expression levels of *BCL2* and *BCLxL* in $CD4^+$ T cells of SLE were significantly higher than those of HC (Figure 3F). Besides, the mRNA expression level of *BCL2* in $CD4^+$ T cells of SLE was positively correlated to the mRNA expression level of *p53* (Figure 3G), and the mRNA expression level of *BCLxL* was positively correlated to the mRNA expression levels of *CD57* and *p53* (Figure 3H).

To explore the underlying mechanisms of senescent CD4$^+$ T cells in the pathogenesis of SLE, we performed bioinformatics analysis in a single-cell sequencing dataset from the GEO database focusing on differentially expressed genes of CD4$^+$CD57$^+$ senescent CD4$^+$ T cells between SLE patients and HCs. We analyzed single-cell sequencing dataset of PBMCs from 7 SLE patients and 5 HCs and performed dimensionality reduction with T-distributed stochastic neighbor embedding (T-SNE), dividing all PBMCs into 21 cell clusters (Figure S2B~~S2C~~ and 3I). We annotated six subgroups: naïve B cells, CD14$^+$ monocytes, CD16$^+$ monocytes, NK cells, CD4$^+$ T cells, and CD8$^+$ T cells (Figure 3J). Finally, we extracted CD4$^+$ T cells and screened the CD4$^+$CD57$^+$ senescent CD4$^+$ T cells from SLE patients and HCs according to the expression of *CD57*, and then performed differential gene analysis in senescent CD4$^+$ T cells between SLE and HCs. The results showed that when compared with the senescent CD4$^+$ T cells of HC, the interferon-stimulated genes (ISGs) and genes related to the type I interferon signaling pathway (such as *IFI27*, *IFI44L*, *BST2*, *LY6E*, *ISG15*, *MX1*, *IFI6*, *IFITM3*, *RGS1*, *IFI44*, *IFITM1*, *EPSTI1*, *Sp100*, *XAF1*, *STAT1*, *BCLAF1*, *PSME2*, *ADAR*, *PSMB9*, *IRF7*, *NT5C3A*, *UBE2L6*, *PSMB2*, *EIF2AK2*, *OAS1*) were significantly upregulated in senescent CD4$^+$ T cells of SLE (Figure 3K).

4. ABT-263 significantly alleviated lupus-like phenotypes in MRL/lpr mice.

In 2015, senolytics, which can selectively eliminate senescent cells, were first mentioned in Aging Cell[12]. Since, studies have shown that senolytics can delay the progression of a variety of aging-related diseases, such as cardiovascular diseases, neurological disorders, liver diseases, kidney diseases, metabolism-related diseases, organ transplantation, and cancer[25]. The BCL-2 protein family inhibitor ABT-263 (also known as navitoclax) was reported to belong to ~~S~~senolytics[26-28]. ABT-263 can initiate the apoptosis of senescent cells by inhibiting BCL-2 and BCL-xL which are upregulated in senescent cells[26, 28]. ABT-263 has been reported to have therapeutic effects in animal models of many diseases such as atherosclerosis, diabetes, liver disease, kidney disease, hematologic disorders, and tumors[29-38]. However, there are no studies on the therapy of eliminating senescent cells in SLE.

Based on our results showing that the CD4$^+$CD57$^+$ senescent T cells were increased in the peripheral blood of SLE patients, particularly, in patients with active disease, we explored whether treatment with the BCL-2 inhibitor, ABT-263, decreased senescent CD4$^+$ T cells. We treated the human PBMCs obtained from both healthy controls and SLE patients with 0, 0.05, 0.5, and 5 μM ABT-263 respectively for 72 hours and then detected the frequency of CD4$^+$CD57$^+$ senescent CD4$^+$ T cells through flow cytometry (Figure 4A). The results showed that both healthy controls (Figure 4B) and SLE patients (Figure 4C) exhibited a significant reduction in the proportion of CD4$^+$CD57$^+$ senescent CD4$^+$ T cells following treatment with 0.5 μM and 5 μM ABT-263. Even more interesting is that even at a low concentration of 0.05 μM ABT-263, there was a decrease in the frequency of CD4$^+$CD57$^+$ senescent CD4$^+$ T cells in SLE patients (Figure 4C), while no significant reduction was observed in healthy controls (Figure 4B). These results demonstrate a high sensitivity of CD4$^+$CD57$^+$ senescent CD4$^+$ T cells in SLE patients to ABT-263.~~there was no difference in the frequency of live cells~~

~~among PBMCs with 0, 0.05, 0.5, and 5 μM ABT-263 treatment (Figure S2D and S2E). However, the 0.5 μM and 5 μM ABT-263 treatment significantly reduced the proportion of $CD4^+CD57^+$ senescent $CD4^+$ T cells and the frequency of $CD4^+CD57^+$ senescent $CD4^+$ T cells in the 5 μM ABT-263 group was slightly lower than that in 0.5 μM (Figure 4B)~~.

Next, we randomized 24 MRL/lpr mice, the most commonly used spontaneous SLE mouse models, into two groups to receive treatment with the ABT-263 group (40 mg/kg ABT-263) or vehicle (equivalent vehicle). The MRL/lpr mice were treated three times a week from 12 weeks until 30 weeks. The survival curve was shown in Figure S2C. We then analyzed the therapeutic effects of ABT-263 on the lupus-like phenotypes of MRL/lpr mice. The results showed that after the 14-week ABT-263 treatment, the level of serum antinuclear antibody (ANA) in MRL/lpr mice was significantly reduced (Figure 4D~~4C~~). The scarred erythema with follicular keratotic plugs and the infiltration of inflammatory cells in H&E staining occurred in one MRL/lpr mouse in the vehicle group, while there were no skin lesions in MRL/lpr mice with ABT-263 treatment (Figure S3A and S3B).

In addition, ABT-263 treatment significantly alleviated renal injury in MRL/lpr mice. The level of urine protein significantly improved after 18 weeks of treatment with ABT-263 (Figure 4E). The results from H&E staining showed increased glomerular volume, glomerular mesangial cell proliferation, and obvious inflammatory cell infiltration in the renal tissue of MRL/lpr mice in the vehicle group (Figure 4F~~4D~~) and the degree of renal lesions was more severe in MRL/lpr mice from vehicle group when compared with MRL/lpr mice from ABT-263 group (Figure 4F~~4D~~). The immunohistochemistry (IHC) staining for C3 and IgG revealed that relatively greater deposition of C3 and IgG occurred in the renal tissue of MRL/lpr mice from the vehicle group when compared with the renal tissue of MRL/lpr mice with ABT-263 treatment (Figure 4F~~5D~~). These results suggested that ABT-263 treatment was associated with fewer renal inflammatory changes.

We found that lymphocyte counts in the spleen and draining lymph nodes (dLNs) were significantly lower in MRL/lpr mice after treatment with ABT-263 when compared with vehicle (Figure 4H~~4G~~). Further, we noted that after ABT-263 treatment, the proportion of Tfh ($CD4^+CXCR5^+PD\text{-}1^+$) cells in the spleen and dLNs of MRL/lpr mice was significantly lower (Figure 4G and I~~4F and H~~), and the frequency of Treg ($CD4^+CD25^+FOXP3^+$) cells in dLNs was significantly higher, the frequency of Treg cells in the spleen was slightly higher when compared with MRL/lpr mice treated with vehicle (Figure 4G and I~~4F and H~~). Also, the frequency of GC B ($B220^+FAS^+GL7^+$) cells in the spleen was significantly lower in MRL/lpr mice with ABT-263 treatment relative to vehicle (Figure 4G and I~~4F and H~~).

5. ABT-263 significantly decreased senescent $CD4^+$ T cells in MRL/lpr mice.

To explore underlying mechanisms of ABT-263 in the MRL/lpr mouse model, we analyzed the frequencies of $CD4^+CD44^{hi}CD62L^-PD\text{-}1^+CD153^+$ senescent $CD4^+$ T cells and $CD19^+CD11C^+T\text{-}bet^+$ age-related B cells (ABCs) in MRL/lpr mice. The results showed that both the frequencies of senescent CD4$^+$ T cells (Figure 5A and S3C5C and S3C) and ABCs (Figure 5B and S3D5D and S3D) were significantly increased in the dLNs and spleen of MRL/lpr mice when compared with the MRL/mpj mice. Notably, we found that the frequencies of senescent CD4$^+$ T cells and ABCs cells in the spleen of MRL/lpr mice were significantly lower in those treated with ABT-263 relative to vehicle (Figure 5C-F5A, 5B, 5E, and 5F). In addition, ABT-263 treatment was associated with significantly lower mRNA levels of markers of cellular senescence including *p16*, *p21*, *p53*, SASP (such as *Il1β* and *Mmp13*), and also anti-apoptotic proteins from the BCL-2 family (*Bcl2* and *Bclxl*) in isolated CD4$^+$ T cells from the dLNs of MRL/lpr mice (Figure 5G-I).

We analyzed the effects of the BCL-2 inhibitor, ABT-263, on the downstream ISGs of senescent CD4$^+$ T cells through RT-qPCR, the results showed that the mRNA expression level of *Stat3* (involved in interferon signaling pathways) in isolated CD4$^+$ T cells from the dLNs of MRL/lpr mice was significantly reduced after the treatment of ABT-263 (Figure 5J); the mRNA expressions of *Stat1* and ISGs (*Ube2l6*, *Bst2*, *Rgs1*, and *Sp100*) in CD4$^+$ T cells from the dLNs of MRL/lpr mice from ABT-263 group showed a trend towards lower expression, however, this did not reach statistical significance (Figure 5K).

6. IL-15 cytokine elevated the frequency of senescent CD4$^+$ T cells and upregulated the expression of BCL-2 and ISGs.

To explore the upstream regulators that elevate CD4$^+$CD57$^+$ senescent CD4$^+$ T cells in

SLE, we cultured human PBMCs in the presence of single cytokine (IL-6, IL-10, IL-15, IL-21, IFN-α, or IFN-γ) stimulation prior to flowcytometric analysis for $CD4^+CD57^+$ senescent $CD4^+$ T cells (Figure 6A). The results showed that compared with PBS, the proportion of senescent $CD4^+$ T cells was significantly increased after 72 hours of incubation in the presence of IL-15 at 20 ng/mL (Figure 6B). Further, IL-15 stimulation at 20 ng/mL resulted in upregulated expression of BCL-2 in $CD4^+$ T cells (Figure 6C and D) and in $CD4^+CD57^+$ senescent $CD4^+$ T cells (Figure 6E and G). In contrast, incubation of PBMCs with cytokines IL-6, IL-10, IL-21, IFN-α, and IFN-γ failed to increase the proportion of senescent $CD4^+$ T cells (Figure S3E). Surprisingly, we found that both the mRNA expression levels of *IL15* and *IL15R* were significantly upregulated in $CD4^+$ T cells of SLE (Figure 6H) and positively correlated to the SLEDAI scores (Figure 6F and I), suggesting a potentially important role of IL-15 in the pathogenesis of SLE.

In addition, we cultured human $CD4^+$ T cells with IL-15 at 20 ng/mL for 72 hours prior to performing RT-qPCR, which showed that the mRNA expression levels of cellular senescence-related genes, such as *CD57*, *p16*, *p21*, *IL6*, *IL8*, *TNFα*, and *IL1β*, were significantly upregulated in $CD4^+$ T cells with IL-15 cytokine stimulation (Figure 6J). Further, stimulation with IL-15 significantly upregulated the mRNA expression levels of *BCL2* and *BCLxL* in $CD4^+$ T cells (Figure 6K). The mRNA expression levels of ISGs, such as *EIF2AK2*, *UBE2L6*, *PSMB9*, *BST2*, *LY6E*, *RGS1*, *NT5C3A*, *Sp100*, *PSME2*, and *IFITM1*, were also significantly upregulated after the 20 ng/mL IL-15 cytokine stimulation (Figure 6L and M).

Thus, in our study, we speculate that IL-15 promotes accumulation of a greater frequency of $CD4^{+}CD57^{+}$ senescent T cells noted in peripheral blood of SLE patients. Our data also suggested that, in this context, IL-15 upregulates the expression of BCL-2 and Bcl-x~~X~~L and ISGs, which may serve to antagonize apoptotic triggers and promote pro-inflammatory function of senescent $CD4^{+}$ T cells whereas treatment with the senolytic, ABT-263, abrogated inflammation in this model of murine lupus, potentially through limiting the accumulation of senescent $CD4^{+}$ T cells (Figure 7).

Discussion

Senescent T cells, characterized by high expression of cell surface markers CD57 and KLRG1 and lack of CD27 and CD28, upregulation of p53 are potent at secreting SASP [39], thereby, contributing to age-associated multimorbidity including the development of atherosclerosis, neurodegenerative diseases, tumors, and autoimmune diseases[39]. However, evidence is limited about the role of senescent $CD4^{+}$ T cells in the pathogenesis of SLE, an autoimmune disease with chronic inflammation affecting several organs including the kidneys (REF). Here, we found that the frequency of $CD4^{+}CD57^{+}$ senescent $CD4^{+}$ T cells was significantly increased in the peripheral blood of patients with SLE, and was positively correlated with the SLEDAI scores, suggesting that senescent $CD4^{+}$ T cells may be involved in the pathogenesis of SLE.

Previous studies have shown that senescent $CD4^{+}$ T cells express Th1 cytokines after stimulation of T cell receptors [40, 41]. We know that, a population of Tfh cells with characteristics of cellular senescence and a potential to contribute to inflammation accumulates with ageing[42]. Here, we found a significant increase in the frequency of senescent Th1 and senescent Tfh-like cells in peripheral blood samples from SLE patients, suggesting that Th1 and Tfh-like senescence may play an important role in SLE.

Currently, our understanding of the precise role of senescent CD4$^+$ T cells in the pathogenesis of SLE is limited. We know that senescent CD4$^+$ T cells upregulate anti-apoptotic BCL-2 family of proteins and resist apoptosis[9-12]. Our results confirmed that senescent CD4$^+$ T cells from SLE patients also upregulate both BCL-2 and BCL-xL, which may explain their persistence. Further, senescent T cells from SLE patients also upregulate ISGs, which taken together with the data derived from bioinformatics analysis of single-cell sequencing data from public databases suggest that senescent T cells from SLE patients are primed to secrete interferons, which play a significant role in the pathogenesis of SLE[43] although precise molecular mechanisms need further elucidation.

We know that IL-15 is a key regulator in the host's defense response to pathogens and is widely expressed in multiple cell types, such as monocytes and macrophages[44]. IL-15 is a growth factor that plays a vital role in the development, homeostasis, and function of T, NK, and NK-T cells by inhibiting apoptosis[44]. Besides, IL-15 can participate in the activation and differentiation of T cells by promoting the production of inflammatory cytokines in dendritic cells and macrophages[44]. Studies have shown that the IL-15 is significantly elevated in the serum of SLE patients and that serum levels of IL-15 are significantly higher in SLE patients with lupus nephritis than those in SLE patients without lupus nephritis[45-47]. Our study showed that the mRNA expression levels of *IL15* and *IL15R* were significantly elevated in peripheral $CD4^+$ T cells of SLE patients and were positively correlated to the SLEDAI score. In recent years, studies have shown that IL-15 can promote the accumulation of senescent $CD8^+CD57^+$ T cells and related to upregulated activity of BCL-2[48, 49]. Our data showing that in the presence of IL-15 senescent $CD4^+$ T cells from patients with SLE significantly upregulate their expressions of BCL-2 and BclXL and also ISGs. Therefore, these data indicated elevated serum IL-15 in SLE patients may promote upregulation of BCL-2 family members and ISGs in senescent $CD4^+$ T cells and contribute to chronic inflammation in SLE.

We know from preclinical studies that ‘senolytics’ represent a plausible therapeutic strategy to target age-related diseases. For example, BCL-2 inhibitors have been reported to be effective in many diseases, such as atherosclerosis, diabetes, and tumors, and can promote the regeneration of kidney, liver, hematopoietic stem cells, and hair follicle stem cells[29-37]. As yet, there are no studies about the use of senolytics for the treatment of SLE. As our data revealed increased prevalence of senescent $CD4^+$ T cells and ABC in the spleen and dLNs of MRL/lpr mice we used ABT-263 treatment to target senescent $CD4^+$ T cells and ABC. In support of our hypothesis, ABT-263 treatment was associated with lower serum ANA titers, reduced severity of kidney injury, and reduced frequency of senescent T cells and ABCs. Further, ABT-263 treatment was associated with significantly lower frequency of Tfh cells in MRL/lpr mice. In this context, we also found that senescent Tfh-like cells were significantly increased in SLE patients.

Conclusion

Taken together, our data indicated that the $CD4^{+}CD57^{+}$ Senescent T cells as promoters of SLE pathogenesis and~~IL-15-mediated accumulation of senescent $CD4^{+}$ T cells through upregulating BCL-2 family and ISGs, promotes lupus-like phenotypes whereas treatment with~~ the BCL-2 inhibitor ABT-263 was associated with reduction in senescent $CD4^{+}$ T cells and ABC and amelioration of autoimmunity in MRL/lpr mice.

Materials and methods

~~1.~~ Human sample collection

All participants provided informed consent according to the declaration of Helsinki and the experimental protocols were approved by the Ethics Committee of the Second Xiangya Hospital of Central South University. All patients with SLE and RA satisfied the criteria for diagnosis according to the ACR/EULAR criteria. At the time of sample collection, patients had no evidence of infections, tumors, or other systemic diseases. Samples were collected from SLE and RA patients attending the Department of Dermatology and Rheumatology of the Second Xiangya Hospital of Central South University. The age-matched and gender-matched healthy controls (HCs) were collected from the Health Management Center of the Second Xiangya Hospital of Central South University. The Systemic Lupus Erythematosus disease activity score

2000 (SLEDAI-2K) was performed to assess the disease activity of SLE patients and we divided SLE patients into inactive SLE (SLEDAI score ≤ 4) and active SLE (SLEDAI score > 4), demographics and clinical data were shown in Table S1A-E.

Human peripheral blood mononuclear cells (PBMCs) isolation and flow cytometry

Human PBMCs were isolated from peripheral blood using Ficoll-Paque Plus (GE healthcare). A total of 2×10^6 lymphocytes were incubated with antibodies against surface markers at 4℃ for 45 minutes in the dark. For transcription factor staining, Foxp3/Transcription Factor Staining Buffer Set (eBioscience) was used to incubate at 4℃ for 1 hour in the dark and then antibodies against transcription factors were incubated at 4℃ for 90 minutes in the dark. We used BD FACSCantoTM II (BD Biosciences) for detection and FlowJo software (Tree Star) for data analysis. Details of antibodies were shown in Table S2.

Human $CD4^+$ T cells Isolation

We separated the Human $CD4^+$ T cells according to the instructions of the $CD4^+$ T Cell Isolation Kit, human (Miltenyi Biotec).

Total RNA isolation and reverse transcription quantitative PCR (RT-qPCR)

Total RNA isolation was performed by using TRIzol reagent (Invitrogen), and the quality and concentration of RNA were detected via NanoDrop spectrophotometer

(ND-2000, Thermo). The cDNA synthesis of total RNA was performed via PrimeScriptTM RT reagent Kit with gDNA Eraser (TaKaRa). The RT-qPCR was performed by using the SYBR Green Premix Ex TaqTM (TaKaRa) and a thermocycler (Bio-Rad CFX ConnectTM). The fold change of target gene expression was defined as $2^{-\Delta\Delta Ct}$ (ΔCt=Ct of target gene-ΔCt of internal reference (GAPDH or β-actin)). Primers of genes were represented in Table S3.

Bioinformatics analysis

The GSE135779 dataset about Single-cell sequencing of PBMCs in 7 SLE patients and 5 HCs was selected in the GEO database and analyzed[50]. The Seurat was used to integrate 12 samples and the quality control was performed according to the ratio of mitochondria and red blood cells. The t-Distributed Stochastic Neighbor Embedding (t-SNE) was used for Dimensionality reduction and the clusters of cells were annotated via SingleR. In the $CD4^+$ T cell population, we defined $CD4^+CD57^+$ as senescent $CD4^+$ T cells according to the expression of *CD57* (B3GAT1). Next, we compared the differential gene expression analysis between the senescent $CD4^+$ T cells of SLE patients and senescent $CD4^+$ T cells of HCs.

Mice

The MRL/lpr mice and MRL/mpj mice were purchased from Beijing Vital River Laboratory Animal Technology Co., Ltd. The mice were housed in the SPF environment at the Laboratory Animal Center of the Second Xiangya Hospital of

Central South University, and all the operations were approved by the Ethics Committee of the Laboratory Animal Society of Central South University. We randomly divided 24 12-week MRL/lpr mice into 2 groups: 12 mice in the ABT-263 group (gavaged with 40 mg/kg ABT-263 (Selleck), three times a week) and 12 mice in the vehicle group (equivalent 0.5% carboxymethyl cellulose sodium (Selleck) solution, three times a week from 12 weeks until 30 weeks).

Sing-cell suspensions of spleen and draining lymph nodes (dLNs) and flow cytometry

The spleen and dLNs of sacrificed mice were ground and filtered to obtain sing-cell suspensions. For surface markers and transcription factor staining, the methods for flow cytometry were as described previously. For intracellular cytokine staining, 2.5× 106 lymphocytes were cultured with 2.5 μL/mL of Leukocyte Activation Cocktail, with BD GolgiPlug™ (BD Biosciences) in at 37 ℃ in a 5% CO_2 incubator for 6 hours， and then 200 μL of Cytofix/Cytoperm reagent (BD Biosciences) was added and incubated at 4℃ for 1 hour in the dark. The antibodies against intracellular cytokines were incubated at 4℃ for 60 minutes in the dark and the BD FACSCantoTM II and FlowJo software were used for detection and analysis. Details of antibodies were shown in Table S4.

Mouse $CD4^+$ T cells Isolation

We separated the Mouse $CD4^+$ T cells of dLNs according to the instructions of the

504 CD4$^+$ T Cell Isolation Kit, mouse (Miltenyi Biotec).

505 **Histopathology and immunohistochemistry (IHC) staining**

506 The skin and kidney tissues of MRL/lpr mice were treated with formalin and paraffin
507 to make sections (4 mm) for histopathology and IHC staining, respectively. For IHC
508 staining, the sections were dewaxed and then performed with protein blocking
509 (PerkinElmer). Then the sections were incubated with primary antibodies (Anti-mouse
510 C3 antibody, Abcam, ab11862; AF488 anti-mouse IgG; Abcam, ab150117) and a
511 second antibody (Abcam). All data was recorded by PerkinElmer Mantra and analyzed
512 by inform software (PerkinElmer). Details of antibodies were shown in Table S4.

513 **Enzyme-linked immunosorbent assay (ELISA)**

514 The serums of MRL/lpr mice were collected at baseline, 8-week treatment, 14-week
515 treatment, and 20-week treatment. The serum ANA (1:100 Dilution) was detected
516 according to the instructor of the Mouse anti-nuclear Antibody (IgG) ELISA Kit
517 (Cusabio). Then the OD value at 450 nm wavelength was detected.

518 **Statistical analysis**

519 The SPSS software was used for statistical analysis and the data were shown as the
520 means ± SEM. Statistical significance (* $p < 0.05$, ** $p < 0.01$, *** $p < 0.001$, and ****
521 $p < 0.0001$) was compared by two-tailed unpaired or paired Student's t-test for two
522 groups. When the data did not conform to a normal distribution or homogeneity of

variance, the two-tailed Mann-Whitney U test was performed. For correlation analysis of two continuous variables, the Spearman rank correlation test was used. The log-rank test was performed for the comparison of the two groups.

Study approval.

All the protocols and operations for human subjects and animals were approved by the Animal Care and Use Committee of the Laboratory Animal Research Center at the Second Xiangya Medical School, Central South University. All human studies were approved by the Ethics Committee of the Second Xiangya Hospital of Central South University. All SLE and RA patients as well as healthy volunteers provided written informed consent.

Reference

1 **Tsokos, G. C.,** Autoimmunity and organ damage in systemic lupus erythematosus. *Nat Immunol* 2020. **21**: 605-614.

2 **Cui, Y., Sheng, Y. and Zhang, X.,** Genetic susceptibility to SLE: recent progress from GWAS. *J Autoimmun* 2013. **41**: 25-33.

3 **Tsokos, G. C.,** Systemic lupus erythematosus. *N Engl J Med* 2011. **365**: 2110-2121.

4 **Costenbader, K. H., Gay, S., Alarcón-Riquelme, M. E., Iaccarino, L. and Doria, A.,** Genes, epigenetic regulation and environmental factors: which is the most relevant in developing autoimmune diseases? *Autoimmun Rev* 2012. **11**: 604-609.

5 **Hoffman, R. W.,** T cells in the pathogenesis of systemic lupus erythematosus. *Clin Immunol* 2004. **113**: 4-13.

6 Gorgoulis, V., Adams, P. D., Alimonti, A., Bennett, D. C., Bischof, O., Bishop, C., Campisi, J., Collado, M., Evangelou, K., Ferbeyre, G., Gil, J., Hara, E., Krizhanovsky, V., Jurk, D., Maier, A. B., Narita, M., Niedernhofer, L., Passos, J. F., Robbins, P. D., Schmitt, C. A., Sedivy, J., Vougas, K., von Zglinicki, T., Zhou, D., Serrano, M. and Demaria, M., Cellular Senescence: Defining a Path

Forward. *Cell* 2019. 179: 813-827.

7 Liu, J. Y., Souroullas, G. P., Diekman, B. O., Krishnamurthy, J., Hall, B. M., Sorrentino, J. A., Parker, J. S., Sessions, G. A., Gudkov, A. V. and Sharpless, N. E., Cells exhibiting strong p16(INK4a) promoter activation in vivo display features of senescence. *Proc Natl Acad Sci U S A* 2019. 116: 2603-2611.

8 Yosef, R., Pilpel, N., Tokarsky-Amiel, R., Biran, A., Ovadya, Y., Cohen, S., Vadai, E., Dassa, L., Shahar, E., Condiotti, R., Ben-Porath, I. and Krizhanovsky, V., Directed elimination of senescent cells by inhibition of BCL-W and BCL-XL. *Nat Commun* 2016. 7: 11190.

9 **Coppé, J. P., Desprez, P. Y., Krtolica, A. and Campisi, J.,** The senescence-associated secretory phenotype: the dark side of tumor suppression. *Annu Rev Pathol* 2010. **5**: 99-118.

10 **Faget, D. V., Ren, Q. and Stewart, S. A.,** Unmasking senescence: context-dependent effects of SASP in cancer. *Nat Rev Cancer* 2019. **19**: 439-453.

11 **Di Micco, R., Krizhanovsky, V., Baker, D. and d'Adda di Fagagna, F.,** Cellular senescence in ageing: from mechanisms to therapeutic opportunities. *Nat Rev Mol Cell Biol* 2021. **22**: 75-95.

12 **Childs, B. G., Durik, M., Baker, D. J. and van Deursen, J. M.,** Cellular senescence in aging and age-related disease: from mechanisms to therapy. *Nat Med* 2015. **21**: 1424-1435.

13 **Lagoumtzi, S. M. and Chondrogianni, N.,** Senolytics and senomorphics: Natural and synthetic therapeutics in the treatment of aging and chronic diseases. *Free Radic Biol Med* 2021. **171**: 169-190.

14 **Palmer, B. E., Mack, D. G., Martin, A. K., Maier, L. A. and Fontenot, A. P.,** CD57 expression correlates with alveolitis severity in subjects with beryllium-induced disease. *J Allergy Clin Immunol* 2007. **120**: 184-191.

15 **Covre, L. P., De Maeyer, R. P. H., Gomes, D. C. O. and Akbar, A. N.,** The role of senescent T cells in immunopathology. *Aging Cell* 2020. **19**: e13272.

16 **Sato, K., Kato, A., Sekai, M., Hamazaki, Y. and Minato, N.,** Physiologic Thymic Involution Underlies Age-Dependent Accumulation of Senescence-Associated CD4(+) T Cells. *J Immunol* 2017. **199**: 138-148.

17 Villanueva-Romero, R., Lamana, A., Flores-Santamaría, M., Carrión, M., Pérez-García, S., Triguero-Martínez, A., Tomero, E., Criado, G., Pablos, J. L., González-Álvaro, I., Martínez, C., Juarranz, Y., Gomariz, R. P. and Gutiérrez-Cañas, I., Comparative Study of Senescent Th Biomarkers in Healthy Donors and Early Arthritis Patients. Analysis of VPAC Receptors and Their Influence. *Cells* 2020. 9.

18 Fessler, J., Husic, R., Schwetz, V., Lerchbaum, E., Aberer, F., Fasching, P., Ficjan, A., Obermayer-Pietsch, B., Duftner, C., Graninger, W., Stradner, M. H. and Dejaco, C., Senescent T-Cells

Promote Bone Loss in Rheumatoid Arthritis. *Front Immunol* 2018. 9: 95.

19 **Yamada, H., Kaibara, N., Okano, S., Maeda, T., Shuto, T., Nakashima, Y., Okazaki, K. and Iwamoto, Y.,** Interleukin-15 selectively expands CD57+ CD28- CD4+ T cells, which are increased in active rheumatoid arthritis. *Clin Immunol* 2007. **124**: 328-335.

20 **Tahir, S., Fukushima, Y., Sakamoto, K., Sato, K., Fujita, H., Inoue, J., Uede, T., Hamazaki, Y., Hattori, M. and Minato, N.,** A CD153+CD4+ T follicular cell population with cell-senescence features plays a crucial role in lupus pathogenesis via osteopontin production. *J Immunol* 2015. **194**: 5725-5735.

21 Shirakawa, K., Yan, X., Shinmura, K., Endo, J., Kataoka, M., Katsumata, Y., Yamamoto, T., Anzai, A., Isobe, S., Yoshida, N., Itoh, H., Manabe, I., Sekai, M., Hamazaki, Y., Fukuda, K., Minato, N. and Sano, M., Obesity accelerates T cell senescence in murine visceral adipose tissue. *J Clin Invest* 2016. 126: 4626-4639.

22 Gosselin, A., Monteiro, P., Chomont, N., Diaz-Griffero, F., Said, E. A., Fonseca, S., Wacleche, V., El-Far, M., Boulassel, M. R., Routy, J. P., Sekaly, R. P. and Ancuta, P., Peripheral blood CCR4+CCR6+ and CXCR3+CCR6+CD4+ T cells are highly permissive to HIV-1 infection. *J Immunol* 2010. 184: 1604-1616.

23 **Yeh, C. H., Finney, J., Okada, T., Kurosaki, T. and Kelsoe, G.,** Primary germinal center-resident T follicular helper cells are a physiologically distinct subset of CXCR5(hi)PD-1(hi) T follicular helper cells. *Immunity* 2022. **55**: 272-289.e277.

24 **Yu, N., Li, X., Song, W., Li, D., Yu, D., Zeng, X., Li, M., Leng, X. and Li, X.,** CD4(+)CD25 (+)CD127 (low/-) T cells: a more specific Treg population in human peripheral blood. *Inflammation* 2012. **35**: 1773-1780.

25 **Kirkland, J. L. and Tchkonia, T.,** Senolytic drugs: from discovery to translation. *J Intern Med* 2020. **288**: 518-536.

26 Zhu, Y., Tchkonia, T., Fuhrmann-Stroissnigg, H., Dai, H. M., Ling, Y. Y., Stout, M. B., Pirtskhalava, T., Giorgadze, N., Johnson, K. O., Giles, C. B., Wren, J. D., Niedernhofer, L. J., Robbins, P. D. and Kirkland, J. L., Identification of a novel senolytic agent, navitoclax, targeting the Bcl-2 family of anti-apoptotic factors. *Aging Cell* 2016. 15: 428-435.

27 Chang, J., Wang, Y., Shao, L., Laberge, R. M., Demaria, M., Campisi, J., Janakiraman, K., Sharpless, N. E., Ding, S., Feng, W., Luo, Y., Wang, X., Aykin-Burns, N., Krager, K., Ponnappan, U., Hauer-Jensen, M., Meng, A. and Zhou, D., Clearance of senescent cells by ABT263 rejuvenates aged hematopoietic stem cells in mice. *Nat Med* 2016. 22: 78-83.

28 **Kirkland, J. L. and Tchkonia, T.,** Cellular Senescence: A Translational Perspective. *EBioMedicine* 2017. **21**: 21-28.

29 Zhu, Y., Tchkonia, T., Pirtskhalava, T., Gower, A. C., Ding, H., Giorgadze, N., Palmer, A. K., Ikeno, Y., Hubbard, G. B., Lenburg, M., O'Hara, S. P., LaRusso, N. F., Miller, J. D., Roos, C. M., Verzosa, G. C., LeBrasseur, N. K., Wren, J. D., Farr, J. N., Khosla, S., Stout, M. B., McGowan, S. J., Fuhrmann-Stroissnigg, H., Gurkar, A. U., Zhao, J., Colangelo, D., Dorronsoro, A., Ling, Y. Y., Barghouthy, A. S., Navarro, D. C., Sano, T., Robbins, P. D., Niedernhofer, L. J. and Kirkland, J. L., The Achilles' heel of senescent cells: from transcriptome to senolytic drugs. *Aging Cell* 2015. 14: 644-658.

30 Xu, M., Pirtskhalava, T., Farr, J. N., Weigand, B. M., Palmer, A. K., Weivoda, M. M., Inman, C. L., Ogrodnik, M. B., Hachfeld, C. M., Fraser, D. G., Onken, J. L., Johnson, K. O., Verzosa, G. C., Langhi, L. G. P., Weigl, M., Giorgadze, N., LeBrasseur, N. K., Miller, J. D., Jurk, D., Singh, R. J., Allison, D. B., Ejima, K., Hubbard, G. B., Ikeno, Y., Cubro, H., Garovic, V. D., Hou, X., Weroha, S. J., Robbins, P. D., Niedernhofer, L. J., Khosla, S., Tchkonia, T. and Kirkland, J. L., Senolytics improve physical function and increase lifespan in old age. *Nat Med* 2018. 24: 1246-1256.

31 **Thompson, P. J., Shah, A., Ntranos, V., Van Gool, F., Atkinson, M. and Bhushan, A.,** Targeted Elimination of Senescent Beta Cells Prevents Type 1 Diabetes. *Cell Metab* 2019. **29**: 1045-1060.e1010.

32 **Basu, A.,** The interplay between apoptosis and cellular senescence: Bcl-2 family proteins as targets for cancer therapy. *Pharmacol Ther* 2021: 107943.

33 Ovadya, Y., Landsberger, T., Leins, H., Vadai, E., Gal, H., Biran, A., Yosef, R., Sagiv, A., Agrawal, A., Shapira, A., Windheim, J., Tsoory, M., Schirmbeck, R., Amit, I., Geiger, H. and Krizhanovsky, V., Impaired immune surveillance accelerates accumulation of senescent cells and aging. *Nat Commun* 2018. 9: 5435.

34 Kolodkin-Gal, D., Roitman, L., Ovadya, Y., Azazmeh, N., Assouline, B., Schlesinger, Y., Kalifa, R., Horwitz, S., Khalatnik, Y., Hochner-Ger, A., Imam, A., Demma, J. A., Winter, E., Benyamini, H., Elgavish, S., Khatib, A. A., Meir, K., Atlan, K., Pikarsky, E., Parnas, O., Dor, Y., Zamir, G., Ben-Porath, I. and Krizhanovsky, V., Senolytic elimination of Cox2-expressing senescent cells inhibits the growth of premalignant pancreatic lesions. *Gut* 2021.

35 Aguayo-Mazzucato, C., Andle, J., Lee, T. B., Jr., Midha, A., Talemal, L., Chipashvili, V., Hollister-Lock, J., van Deursen, J., Weir, G. and Bonner-Weir, S., Acceleration of β Cell Aging Determines Diabetes and Senolysis Improves Disease Outcomes. *Cell Metab* 2019. 30: 129-142.e124.

36 Garrido, A. M., Kaistha, A., Uryga, A. K., Oc, S., Foote, K., Shah, A., Finigan, A., Figg, N., Dobnikar, L., Jørgensen, H. and Bennett, M., Efficacy and limitations of senolysis in atherosclerosis. *Cardiovasc Res* 2021.

37 Mylonas, K. J., O'Sullivan, E. D., Humphries, D., Baird, D. P., Docherty, M. H., Neely, S. A., Krimpenfort, P. J., Melk, A., Schmitt, R., Ferreira-Gonzalez, S., Forbes, S. J., Hughes, J. and Ferenbach, D. A., Cellular senescence inhibits renal regeneration after injury in mice, with senolytic treatment promoting repair. *Sci Transl Med* 2021. 13.

38 **Shahbandi, A., Rao, S. G., Anderson, A. Y., Frey, W. D., Olayiwola, J. O., Ungerleider, N. A. and Jackson, J. G.,** BH3 mimetics selectively eliminate chemotherapy-induced senescent cells and improve response in TP53 wild-type breast cancer. *Cell Death Differ* 2020. **27**: 3097-3116.

39 **Akbar, A. N., Henson, S. M. and Lanna, A.,** Senescence of T Lymphocytes: Implications for Enhancing Human Immunity. *Trends Immunol* 2016. **37**: 866-876.

40 **Kared, H., Martelli, S., Ng, T. P., Pender, S. L. and Larbi, A.,** CD57 in human natural killer cells and T-lymphocytes. *Cancer Immunol Immunother* 2016. **65**: 441-452.

41 Desdín-Micó, G., Soto-Heredero, G., Aranda, J. F., Oller, J., Carrasco, E., Gabandé-Rodríguez, E., Blanco, E. M., Alfranca, A., Cussó, L., Desco, M., Ibañez, B., Gortazar, A. R., Fernández-Marcos, P., Navarro, M. N., Hernaez, B., Alcamí, A., Baixauli, F. and Mittelbrunn, M., T cells with dysfunctional mitochondria induce multimorbidity and premature senescence. *Science* 2020. 368: 1371-1376.

42 Almanan, M., Raynor, J., Ogunsulire, I., Malyshkina, A., Mukherjee, S., Hummel, S. A., Ingram, J. T., Saini, A., Xie, M. M., Alenghat, T., Way, S. S., Deepe, G. S., Jr., Divanovic, S., Singh, H., Miraldi, E., Zajac, A. J., Dent, A. L., Hölscher, C., Chougnet, C. and Hildeman, D. A., IL-10-producing Tfh cells accumulate with age and link inflammation with age-related immune suppression. *Sci Adv* 2020. 6: eabb0806.

43 **Jiang, J., Zhao, M., Chang, C., Wu, H. and Lu, Q.,** Type I Interferons in the Pathogenesis and Treatment of Autoimmune Diseases. *Clin Rev Allergy Immunol* 2020. **59**: 248-272.

44 **Patidar, M., Yadav, N. and Dalai, S. K.,** Interleukin 15: A key cytokine for immunotherapy. *Cytokine Growth Factor Rev* 2016. **31**: 49-59.

45 **Zhu, H., Mi, W., Luo, H., Chen, T., Liu, S., Raman, I., Zuo, X. and Li, Q. Z.,** Whole-genome transcription and DNA methylation analysis of peripheral blood mononuclear cells identified aberrant gene regulation pathways in systemic lupus erythematosus. *Arthritis Res Ther* 2016. **18**: 162.

46 Aringer, M., Stummvoll, G. H., Steiner, G., Köller, M., Steiner, C. W., Höfler, E., Hiesberger, H., Smolen, J. S. and Graninger, W. B., Serum interleukin-15 is elevated in systemic lupus erythematosus. *Rheumatology (Oxford)* 2001. 40: 876-881.

47 Pacheco-Lugo, L., Sáenz-García, J., Navarro Quiroz, E., González Torres, H., Fang, L., Díaz-Olmos, Y., Garavito de Egea, G., Egea Bermejo, E. and Aroca Martínez, G., Plasma cytokines as potential biomarkers of kidney damage in patients with systemic lupus erythematosus. *Lupus* 2019. 28: 34-43.

48 **Le Priol, Y., Puthier, D., Lécureuil, C., Combadière, C., Debré, P., Nguyen, C. and Combadière, B.,** High cytotoxic and specific migratory potencies of senescent CD8+ CD57+ cells in HIV-infected and uninfected individuals. *J Immunol* 2006. **177**: 5145-5154.

49 Morris, S. R., Chen, B., Mudd, J. C., Panigrahi, S., Shive, C. L., Sieg, S. F., Cameron, C. M., Zidar, D. A., Funderburg, N. T., Younes, S. A., Rodriguez, B., Gianella, S., Lederman, M. M. and Freeman, M. L., Inflammescent CX3CR1+CD57+CD8+ T cells are generated and expanded by IL-15. *JCI Insight* 2020. 5.

50 Nehar-Belaid, D., Hong, S., Marches, R., Chen, G., Bolisetty, M., Baisch, J., Walters, L., Punaro, M., Rossi, R. J., Chung, C. H., Huynh, R. P., Singh, P., Flynn, W. F., Tabanor-Gayle, J. A., Kuchipudi, N., Mejias, A., Collet, M. A., Lucido, A. L., Palucka, K., Robson, P., Lakshminarayanan, S., Ramilo, O., Wright, T., Pascual, V. and Banchereau, J. F., Mapping systemic lupus erythematosus heterogeneity at the single-cell level. *Nat Immunol* 2020. 21: 1094-1106.

Figure legend

Figure 1. The frequency of $CD4^{+}CD57^{+}$ senescent $CD4^{+}$ T cells in SLE patients was significantly elevated and positively correlated with disease activity.

Figure 2. Increased frequency of $CD57^{+}$ senescent Tfh-like cells in SLE patients.

Figure 3. Increased expressions of BCL-2 and ISGs in senescent $CD4^{+}$ T cells of SLE.

Figure 4. The senolytics ABT-263 significantly alleviated the lupus-like phenotypes in MRL/lpr mice.

Figure 5. Treatment with ABT-263 significantly reduced the senescent $CD4^{+}$ T cells in MRL/lpr mice.

Figure 6. IL-15 cytokine elevated the frequency of senescent $CD4^{+}$ T cells and upregulated the expression of BCL-2 and ISGs.

Figure 7. The mechanisms of IL-15-triggered $CD4^{+}$ T cell senescence in the progression of SLE.

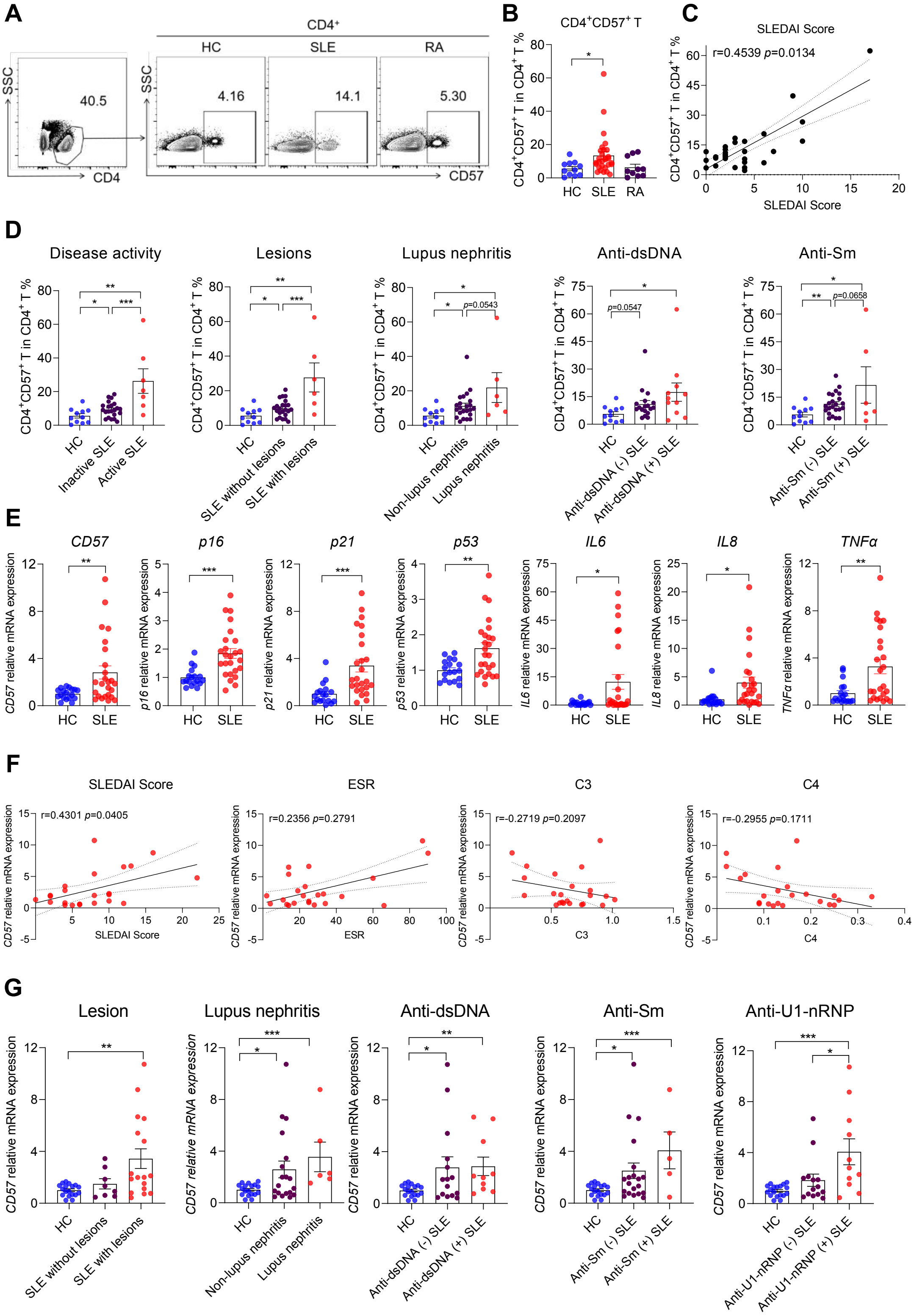

Figure 1. The frequency of $CD4^+CD57^+$ senescent $CD4^+$ T cells in SLE patients was significantly elevated and positively correlated with disease activity.

A-B. Representative flow diagrams of gating and statistical analysis for $CD4^+CD57^+$ senescent $CD4^+$ T cells in $CD4^+$ T cells from peripheral blood of SLE patients (n = 29), RA patients (n = 10), and HCs (n = 11). C. Correlation between the frequency of $CD4^+CD57^+$ senescent $CD4^+$ T cells and the SLEDAI score in SLE patients (n = 29). D. Statistical analysis of the proportion of $CD4^+CD57^+$ senescent $CD4^+$ T cells in distinct SLE patient groups and HCs. E. Comparison of mRNA expression levels of *CD57*, *p16*, *p21*, *p53*, *IL6*, *IL8*, and *TNFα* in peripheral $CD4^+$ T cells between SLE patients (n = 25) and HCs (n = 18). F. Correlation of the mRNA expression levels of *CD57* of peripheral $CD4^+$ T cells with SLEDAI score, ESR, C3, and C4 in SLE patients (n = 23). G. Statistical analysis of the mRNA expression levels of *CD57* of the peripheral $CD4^+$ T cells in distinct SLE patient groups and HCs. Horizontal bars represent the mean ± SEM. * $p < 0.05$, ** $p < 0.01$, *** $p < 0.001$, and r = spearman rank sum correlation coefficient.

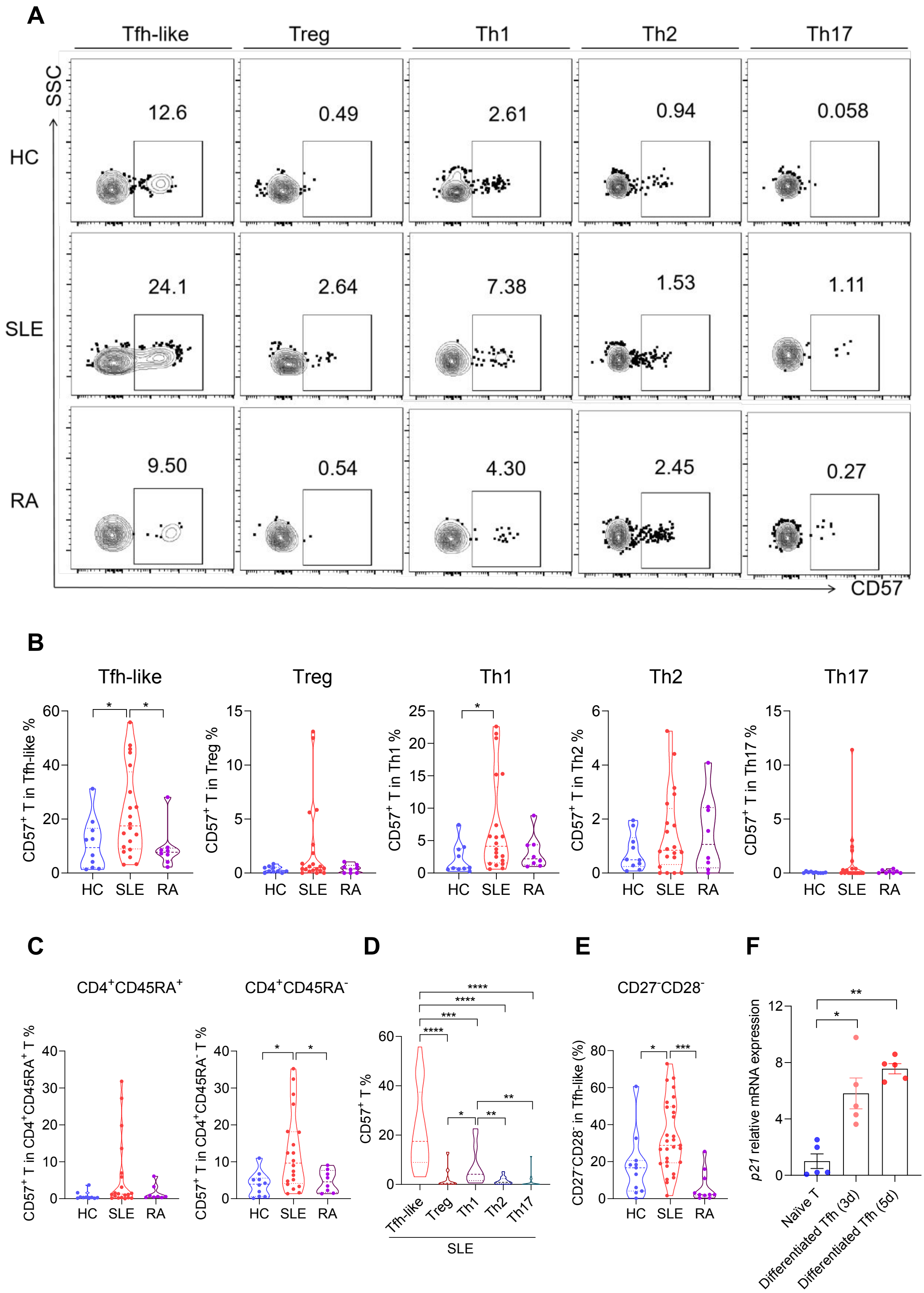

Figure 2. Increased frequency of $CD57^+$ senescent Tfh-like cells in SLE patients.

A-B. Representative flow diagrams and statistical analysis of $CD57^+$ senescent T cells subsets (Tfh-like, Treg, Th1, Th2, and Th17 cells) detectable in peripheral blood of SLE patients (n = 20), RA patients (n = 8), and HCs (n = 10). C. Statistical analysis of the frequency of $CD57^+$ T cells in $CD4^+CD45RA^+$ T and $CD4^+CD45RA^-$ T cells from peripheral blood of SLE patients (n = 20), RA patients (n = 8), and HCs (n = 10). D. Comparison of the frequency of $CD57^+$ senescent T cell subsets (Tfh-like, Treg, Th1, Th2, and Th17) from SLE patients (n = 20). E. Statistical analysis of the frequency of $CD27^-CD28^-$ T cells in Tfh-like cells from SLE patients (n = 29), RA patients (n = 10), and HCs (n = 11). F. Comparison of mRNA expression levels of *p21* among naïve $CD4^+$ T cells (n = 5), differentiated Tfh cells (on day 3) (n = 5), and differentiated Tfh cells (on day 5) (n = 5). Horizontal bars represent the mean ± SEM. * $p < 0.05$, ** $p < 0.01$, *** $p < 0.001$, and **** $p < 0.0001$.

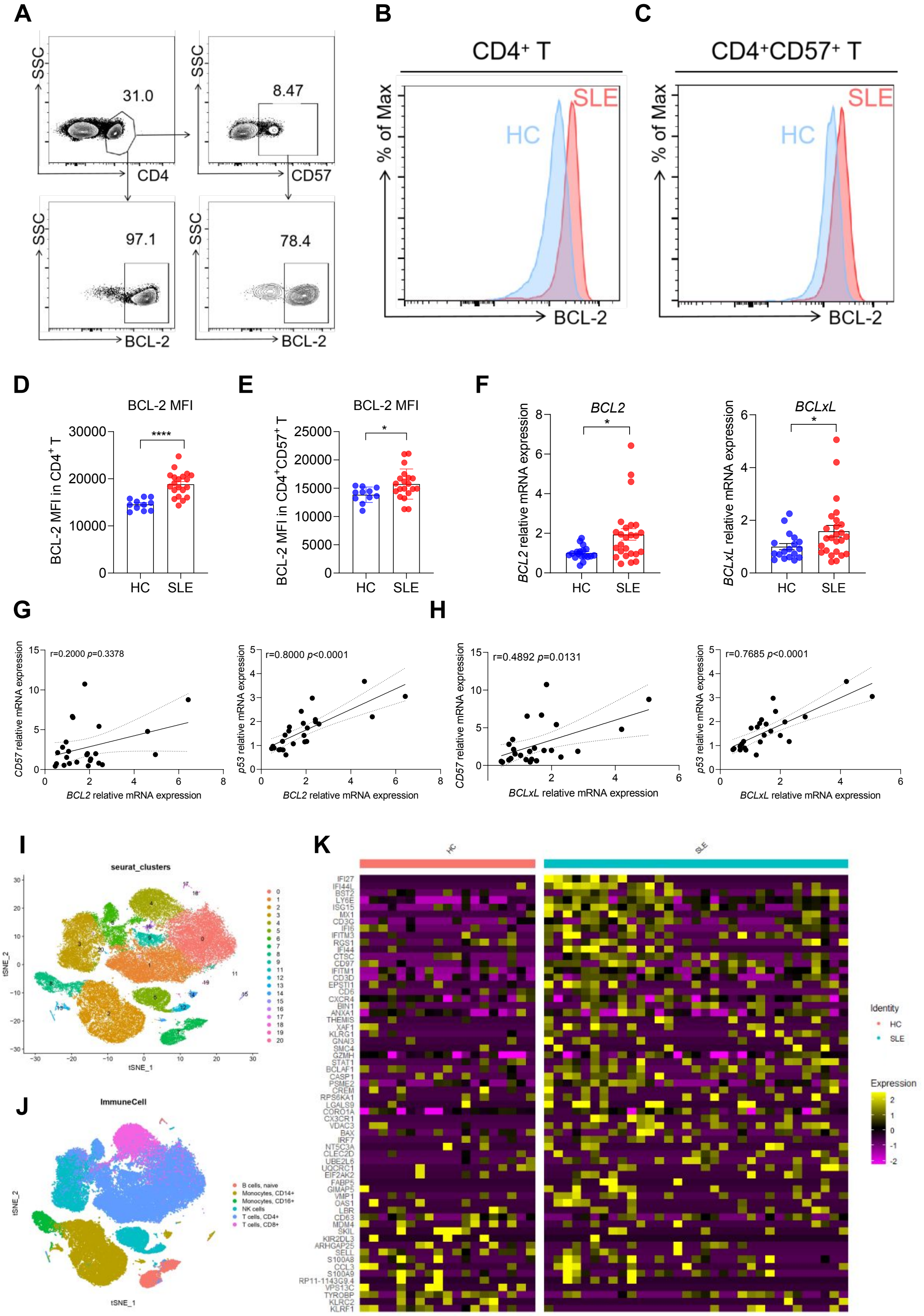

Figure 3. Increased expressions of BCL-2 and ISGs in senescent CD4⁺ T cells of SLE.

A-C. Representative flow diagrams of BCL-2 in $CD4^+$ T cells and $CD4^+CD57^+$ senescent $CD4^+$ T cells from peripheral blood of SLE patients and HCs. D-E. Statistical analysis of the MFI of BCL-2 in $CD4^+$ T cells and senescent $CD4^+$ T cells of SLE patients (n = 20) and HCs (n = 11). F. The comparison of mRNA expression levels of *BCL2* and *BCLxL* between the peripheral blood $CD4^+$ T cells of SLE patients (n = 25) and HCs (n = 18). G. The correlation of the mRNA expression levels of *BCL2* of the peripheral $CD4^+$ T cells with the mRNA expression levels of *CD57* and *p53* in SLE patients (n = 25). H. The correlation of the mRNA expression levels of BCL-xL of the peripheral $CD4^+$ T cells with the mRNA expression levels of *CD57* and *p53* in SLE patients (n = 25). I. The single-cell dataset of PBMCs from peripheral blood of SLE patients (n = 7) and HCs (n = 5) and dimensionality reduction with T-SNE show 21 cell clusters. J. Six subgroups were annotated from the single-cell data of PBMCs from the peripheral blood of SLE patients (n = 7) and HCs (n = 5). K. The differential gene analysis of the peripheral $CD4^+CD57^+$ senescent $CD4^+$ T cells between SLE patients (n = 7) and HCs (n = 5). Horizontal bars represent the mean ± SEM. * $p < 0.05$, **** $p < 0.0001$, and r = spearman rank sum correlation coefficient.

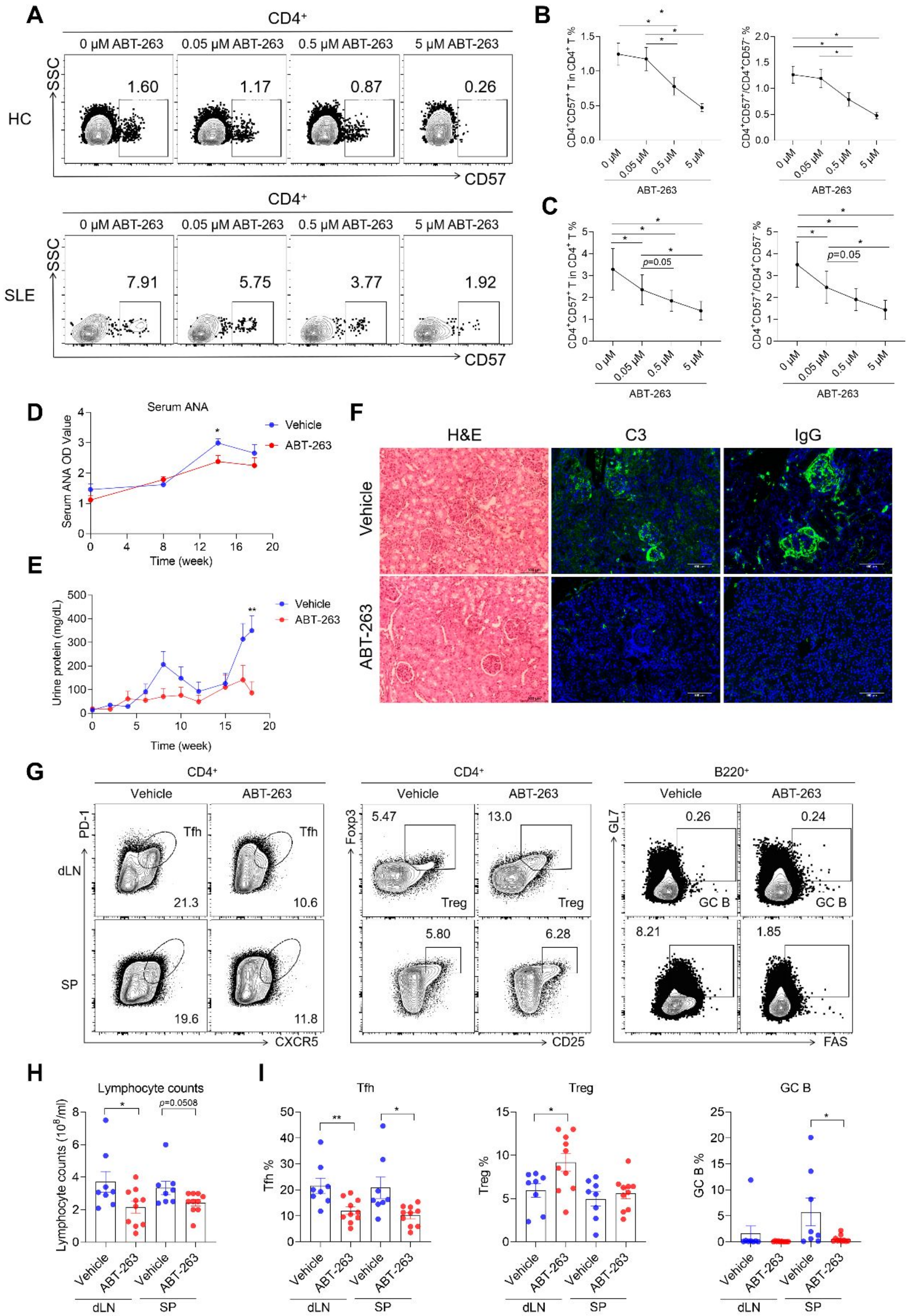
A
CD4+
0 μM ABT-263
0.05 μM ABT-263
0.5 μM ABT-263
5 μM ABT-263
SSC
HC
1.60
1.17
0.87
0.26
CD57
SLE
7.91
5.75
3.77
1.92
B
C
ABT-263
p=0.05
D
Serum ANA
Serum ANA OD Value
Time (week)
Vehicle
E
Urine protein (mg/dL)
F
H&E
C3
IgG
G
CD4+
B220+
PD-1
Tfh
dLN
SP
21.3
10.6
19.6
11.8
CXCR5
Foxp3
5.47
13.0
Treg
5.80
6.28
CD25
GL7
0.26
0.24
GC B
8.21
1.85
FAS
H
Lymphocyte counts
p=0.0508
I
Tfh
Tfh %
Treg
Treg %
GC B
GC B %

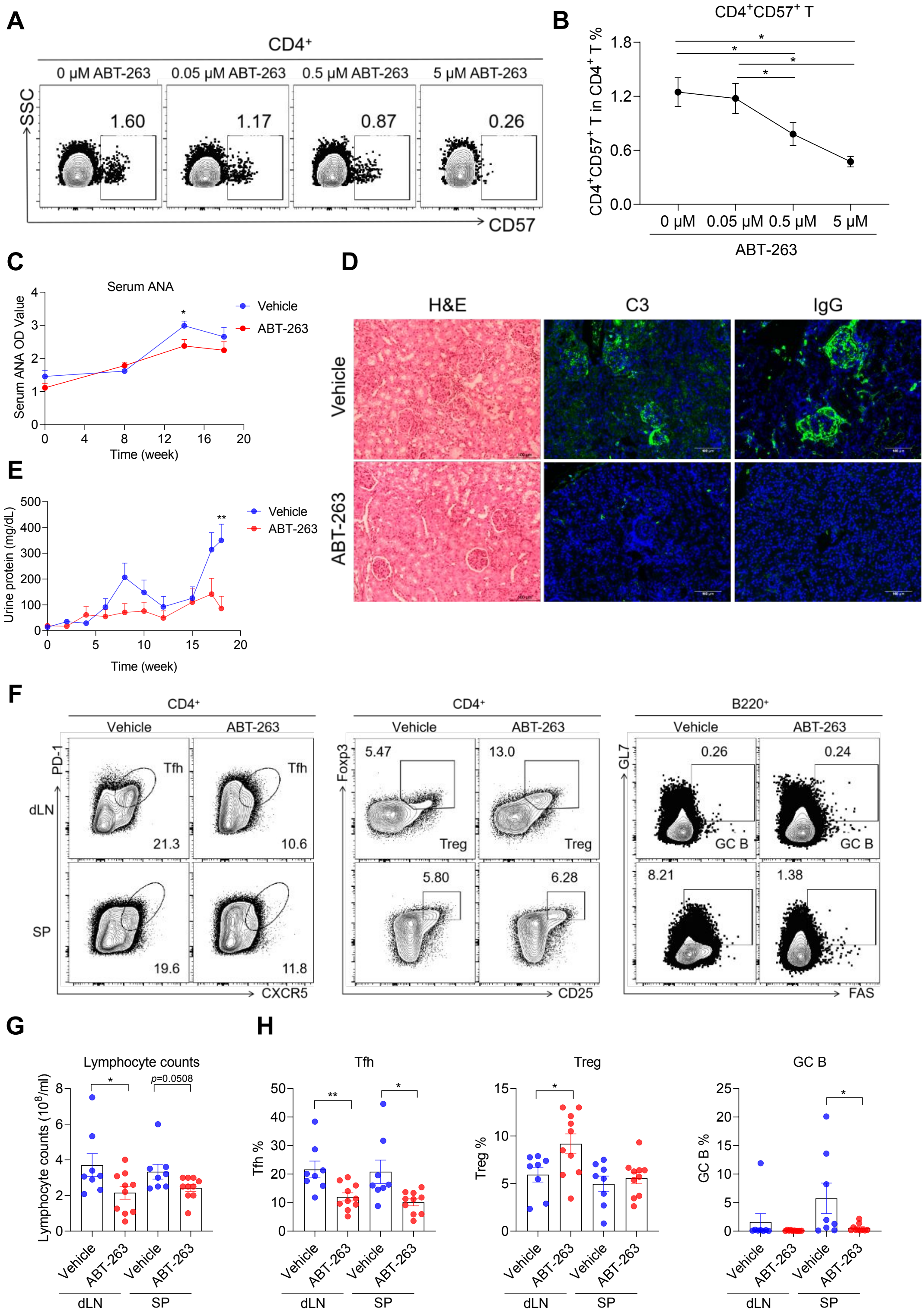

Figure 4. The senolytics ABT-263 significantly alleviated the lupus-like phenotypes in MRL/lpr mice.

A. Representative flow diagrams and statistical analysis of CD4$^+$CD57$^+$ senescent CD4$^+$ T cells in CD4$^+$ T cells from human PBMC obtained from both healthy controls and SLE patients stimulated with 0, 0.05, 0.5, and 5 μM respectively for 72 hours. B-C. Statistical analysis of CD4$^+$CD57$^+$ senescent CD4$^+$ T cells in CD4$^+$ T cells from human PBMC obtained from both healthy controls (n = 6) and SLE patients (n=11) stimulated with 0, 0.05, 0.5, and 5 μM respectively for 72 hours. D. Comparison of the level of serum ANA of MRL/lpr mice treated with ABT-263 (n = 10) or vehicle (n = 8). E. Comparison of the level of urine protein of MRL/lpr mice treated with ABT-263 (n = 10) or vehicle (n = 8). F. Comparison of the H&E staining (× 200) and IHC staining for C3 (× 200) and IgG (× 200) of renal tissues of MRL/lpr mice treated with ABT-263 or vehicle. G-I. Representative flow diagrams and statistical analysis of the lymphocyte counts, the frequency of ~~A-B. Representative flow diagrams and statistical analysis of CD4$^+$CD57$^+$ senescent CD4$^+$ T cells in CD4$^+$ T cells from human PBMC (n = 6) stimulated with 0, 0.05, 0.5, and 5 μM respectively for 72 hours. C. Comparison of the level of serum ANA of MRL/lpr mice treated with ABT-263 (n = 10) or vehicle (n = 8). D. Comparison of the H&E staining (× 200) and IHC staining for C3 (× 200) and IgG (× 200) of renal tissues of MRL/lpr mice treated with ABT-263 or vehicle. E. Comparison of the level of urine protein of MRL/lpr mice treated with ABT-263 (n = 10) or vehicle (n = 8). F-H. Representative flow diagrams and statistical analysis of the lymphocyte counts, the frequency of~~ Tfh (CD4$^+$CXCR5$^+$PD-1$^+$), Treg (CD4$^+$CD25$^+$FOXP3$^+$), and GC B (B220$^+$FAS$^+$GL7$^+$) cells from the spleen and dLNs of MRL/lpr mice treated with ABT-263 (n = 10) or vehicle (n = 8). Horizontal bars represent the mean ± SEM. * $p < 0.05$ and ** $p < 0.01$.

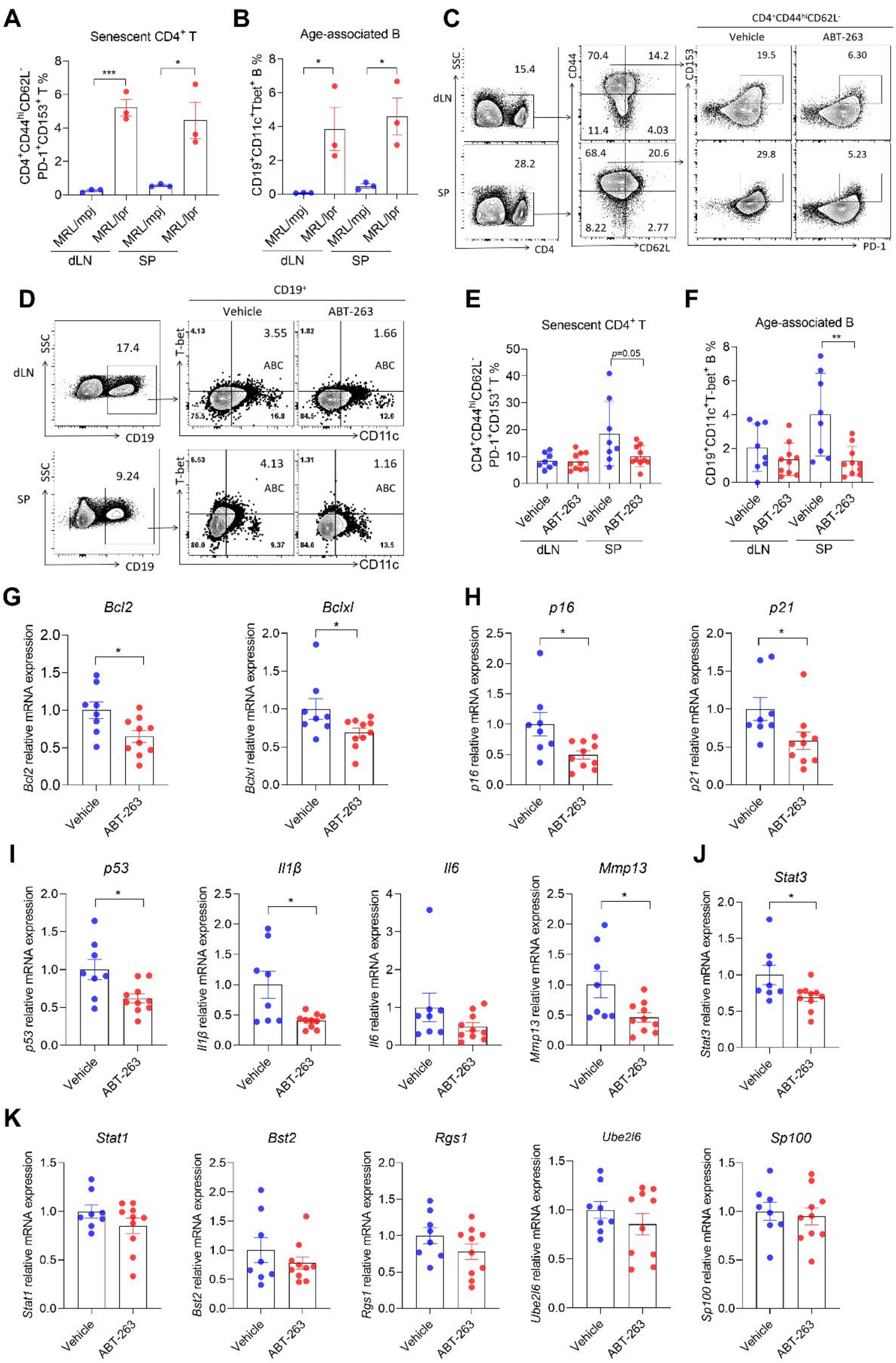

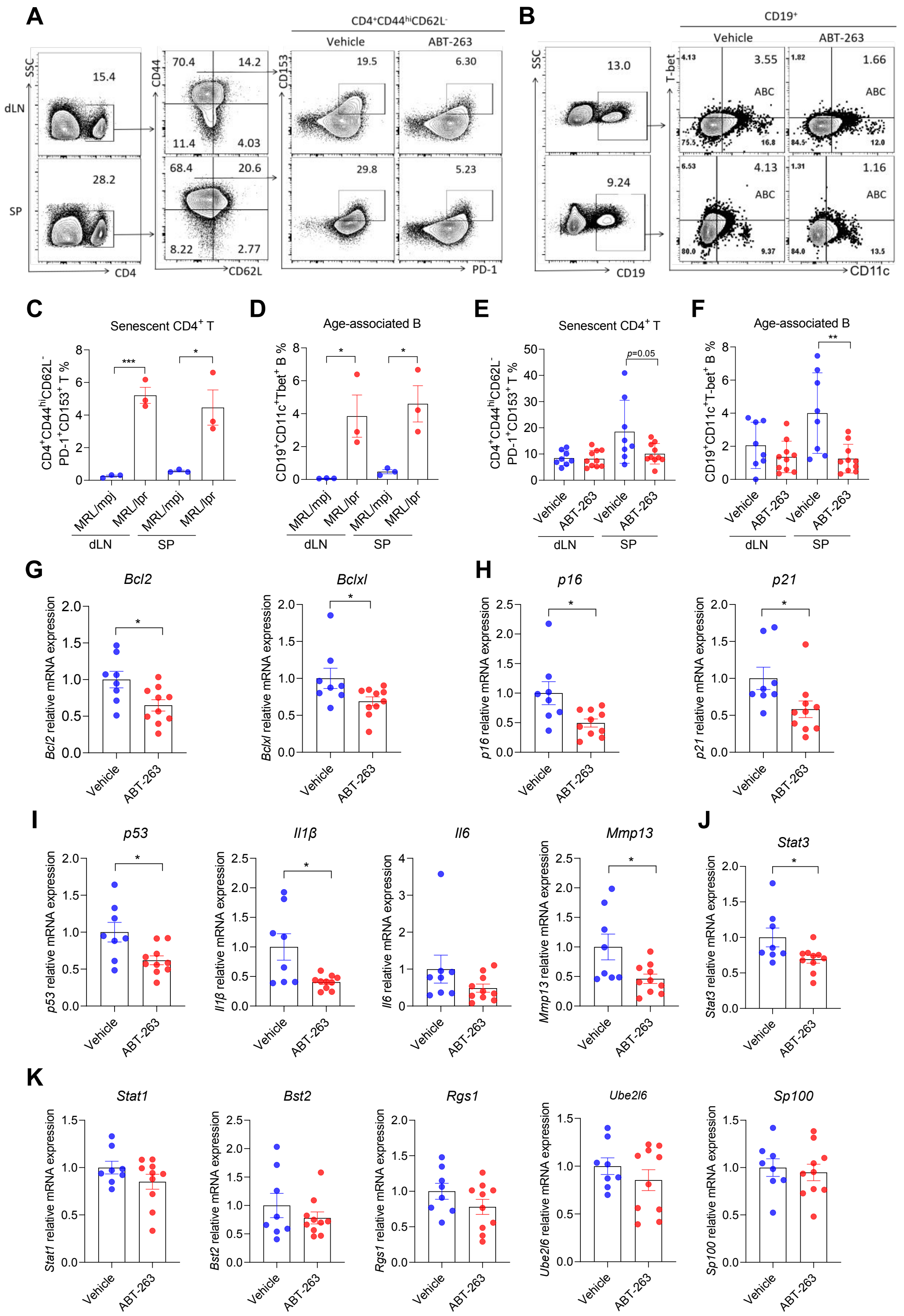

Figure 5. Treatment with ABT-263 significantly reduced the senescent CD4+ T cells in MRL/lpr mice.

A-B. Statistical analysis of senescent CD4$^+$ T cells (CD4$^+$CD44^{hi}CD62L$^-$PD-1$^+$CD153$^+$) and ABC (CD19$^+$CD11c$^+$T-bet$^+$) from the spleen and dLNs of MRL/lpr mice (n = 3) and MRL/mpj mice (n = 3). C-D. Representative flow diagrams of the frequency of senescent CD4$^+$ T cells and ABC from the spleen and dLNs of MRL/lpr mice gavaged with ABT-263 or vehicle. E-F. Statistical analysis of senescent CD4$^+$ T cells and ABC from the spleen and dLNs of MRL/lpr mice treated with ABT-263 (n = 10) or vehicle (n = 8). ~~A-B. Representative flow diagrams of the frequency of senescent CD4$^+$ T cells (CD4$^+$CD44^{hi}CD62L$^-$PD-1$^+$CD153$^+$) and ABC (CD19$^+$CD11c$^+$T-bet$^+$) from the spleen and dLNs of MRL/lpr mice gavaged with ABT-263 or vehicle. C-D. Statistical analysis of senescent CD4$^+$ T cells (CD4$^+$CD44^{hi}CD62L$^-$PD-1$^+$CD153$^+$) and ABC (CD19$^+$CD11c$^+$T-bet$^+$) from the spleen and dLNs of MRL/lpr mice (n = 3) and MRL/mpj mice (n = 3). E-F. Statistical analysis of senescent CD4$^+$ T cells (CD4$^+$CD44^{hi}CD62L$^-$PD-1$^+$CD153$^+$) and ABC (CD19$^+$CD11c$^+$T-bet$^+$) from the spleen and dLNs of MRL/lpr mice treated with ABT-263 (n = 10) or vehicle (n = 8).~~ G-I. Comparison of mRNA expression levels of *Bcl2*, *Bclxl*, *p16*, *p21*, *p53*, *Il1β*, *Il6*, and *Mmp13* of CD4$^+$ T cells from the dLN of MRL/lpr mice treated with ABT-263 (n = 10) or vehicle (n = 8). J-K. Comparison of the mRNA expression levels of *Stat1*, *Stat3*, *Ube2l6*, *Bst2*, *Rgs1*, and *Sp100* in CD4$^+$ T cells from the dLNs of MRL/lpr mice treated with ABT-263 (n = 10) or vehicle (n = 8). Horizontal bars represent the mean ± SEM. * $p < 0.05$, ** $p < 0.01$, and *** $p < 0.001$.

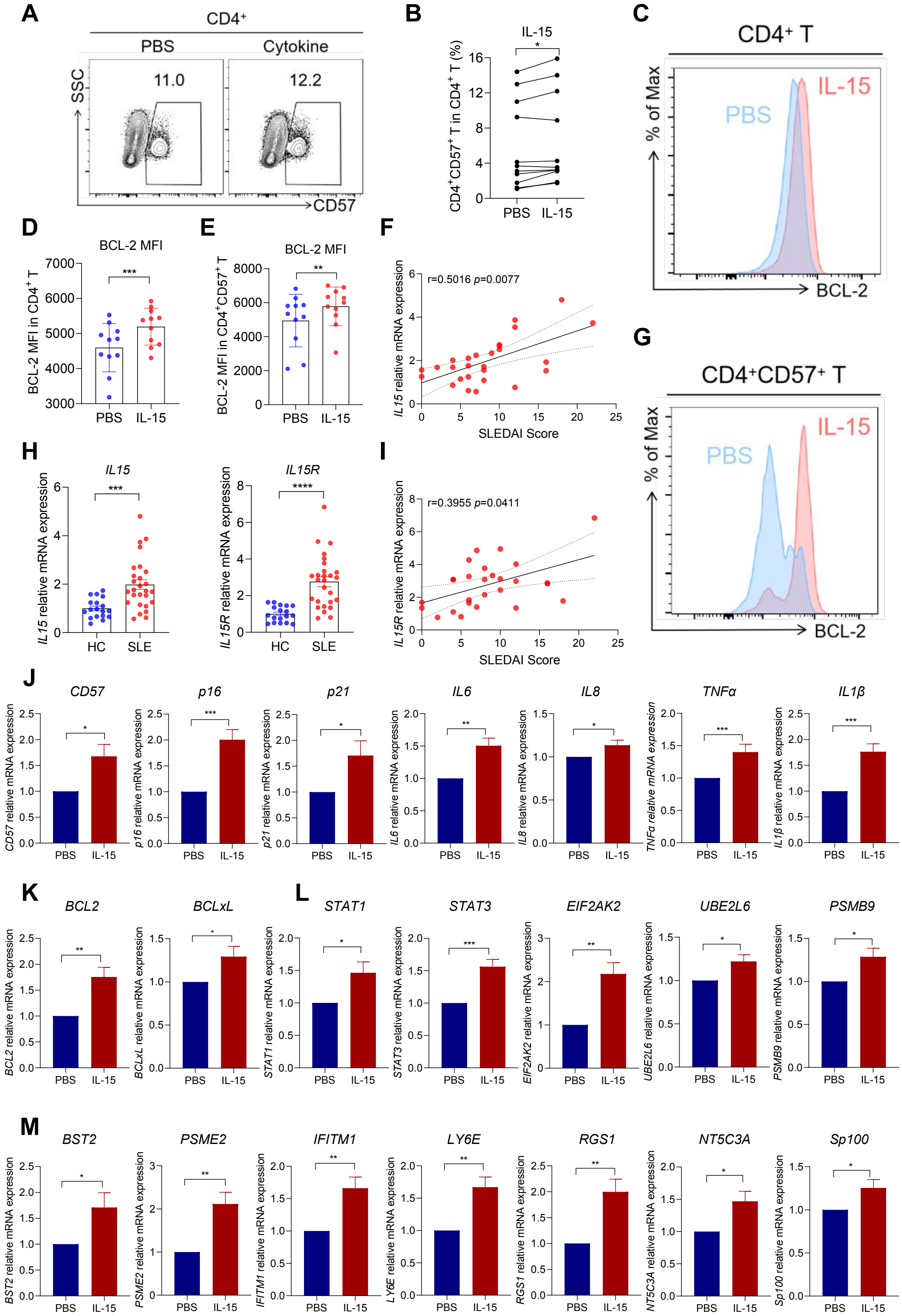

Figure 6. IL-15 cytokine elevated the frequency of senescent CD4+ T cells and upregulated the expression of BCL-2 and ISGs.

A. Representative flow diagrams of $CD4^+CD57^+$ senescent $CD4^+$ T cells in $CD4^+$ T cells from PBMC stimulated with cytokine or PBS. B. Statistical analysis of the frequency of $CD4^+CD57^+$ senescent $CD4^+$ T cells in $CD4^+$ T cells from PBMC stimulated with 20 ng/mL IL-15 (n = 11) or PBS (n = 11). C. Representative flow diagrams of BCL-2 in $CD4^+$ T cells from PBMC stimulated with 20 ng/mL IL-15 (n = 11) or PBS (n = 11). D-E. Statistical analysis of the MFI of BCL-2 in $CD4^+$ T cells and senescent $CD4^+$ T cells from PBMC stimulated with 20 ng/mL IL-15 (n = 11) or PBS (n = 11). F. Correlation of the mRNA expression levels of *IL15* of the peripheral $CD4^+$ T cells with SLEDAI score in SLE patients (n = 27). G. Representative flow diagrams of BCL-2 in $CD4^+CD57^+$ senescent $CD4^+$ T cells from PBMC stimulated with 20 ng/mL IL-15 (n = 11) or PBS (n = 11). H. Comparison of mRNA expression levels of *IL15* and *IL15R* between the peripheral $CD4^+$ T cells of SLE patients (n = 27) and HCs (n = 18). I. Correlation of the mRNA expression levels of *IL15R* of the peripheral $CD4^+$ T cells with SLEDAI score in SLE patients (n = 27). J-M. Comparison of mRNA expression levels of *CD57*, *p16*, *p21*, *IL6*, *IL8*, *TNFα*, *IL1β*, *BCL2*, *BCLxL*, *EIF2AK2*, *UBE2L6*, *PSMB9*, *BST2*, *LY6E*, *RGS1*, *NT5C3A*, *Sp100*, *PSME2* and *IFITM1* of $CD4^+$ T cells with the stimulation of 20 ng/mL IL-15 (n = 6) or PBS (n = 6). Horizontal bars represent the mean ± SEM. * $p < 0.05$, ** $p < 0.01$, *** $p < 0.001$, **** $p < 0.0001$, and r = spearman rank sum correlation coefficient.

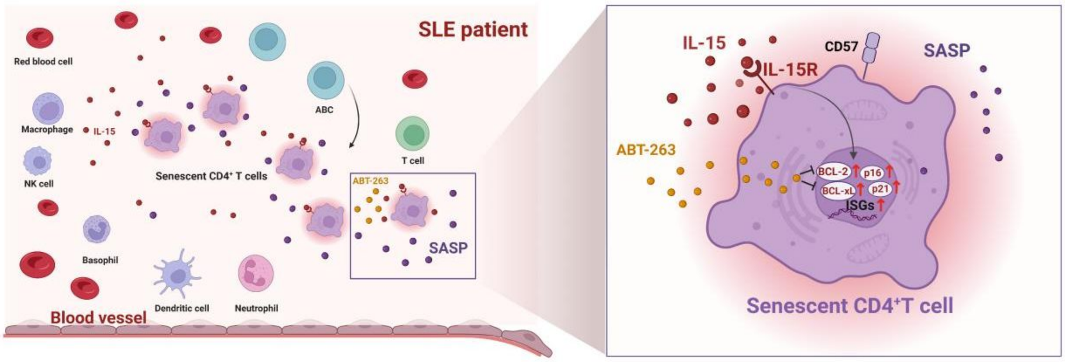

Figure 7. The mechanisms of CD4⁺CD57⁺ Senescent T cells~~IL-15-triggered CD4⁺ T cell senescence~~ in the progression of SLE.

The IL-15-mediated CD4⁺ T cell senescence may be implicated in the progression of SLE by potentially upregulating the BCL-2 family and ISGs~~accelerates the progression of SLE through upregulating the BCL-2 family and ISGs~~ whereas treatment with the BCL-2 inhibitor, ABT-263, eliminated senescent CD4⁺ T cells and alleviated lupus-like phenotypes.

Supplemental file

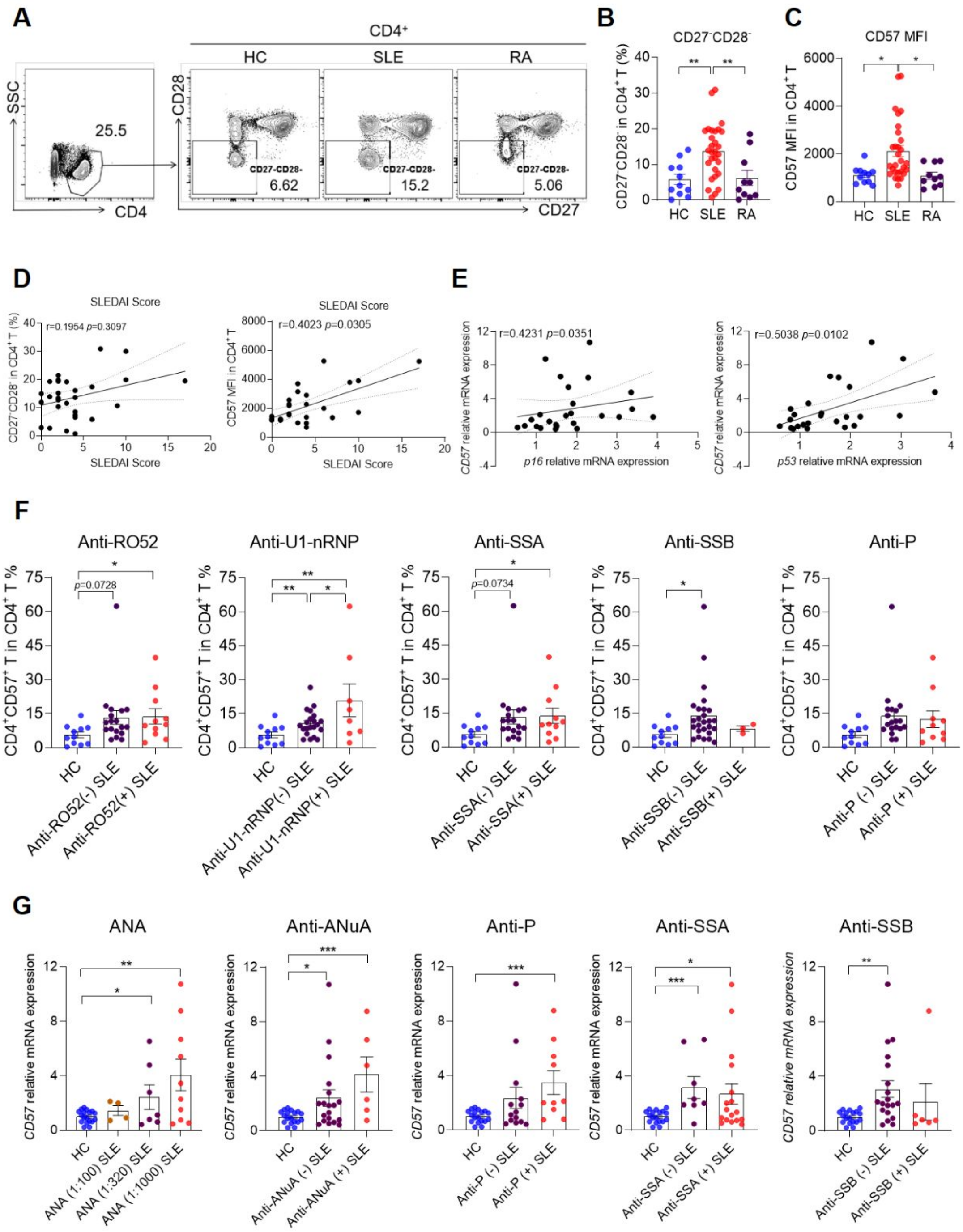

Figure S1.

A-B. Representative flow diagrams of gating and statistical analysis for $CD4^{+}CD27^{-}CD28^{-}$ T cells in $CD4^{+}$ T cells from peripheral blood of SLE patients (n = 29), RA patients (n = 10), and HCs (n = 11). **C.** Statistical analysis of the MFI of CD57 in $CD4^{+}$ T cells from peripheral blood of SLE patients (n = 29), RA patients (n = 10), and HCs (n = 11). **D**. Correlation of the frequency of $CD27^{-}CD28^{-}$ cells and the MFI of CD57 in $CD4^{+}$ T cells with the SLEDAI score in SLE patients (n = 29). **E.** Correlation of the mRNA expression levels of p16 and p53 in $CD4^{+}$ T cells with the mRNA expression levels of CD57 in SLE patients (n = 29). **F-G**. Statistical analysis of the proportion of senescent $CD4^{+}$ T cells and the mRNA expression levels of CD57 of the $CD4^{+}$ T cells in distinct SLE patient groups and HCs. Horizontal bars represent the mean ± SEM. * $p < 0.05$, ** $p < 0.01$, *** $p < 0.001$, and r = spearman rank sum correlation coefficient.

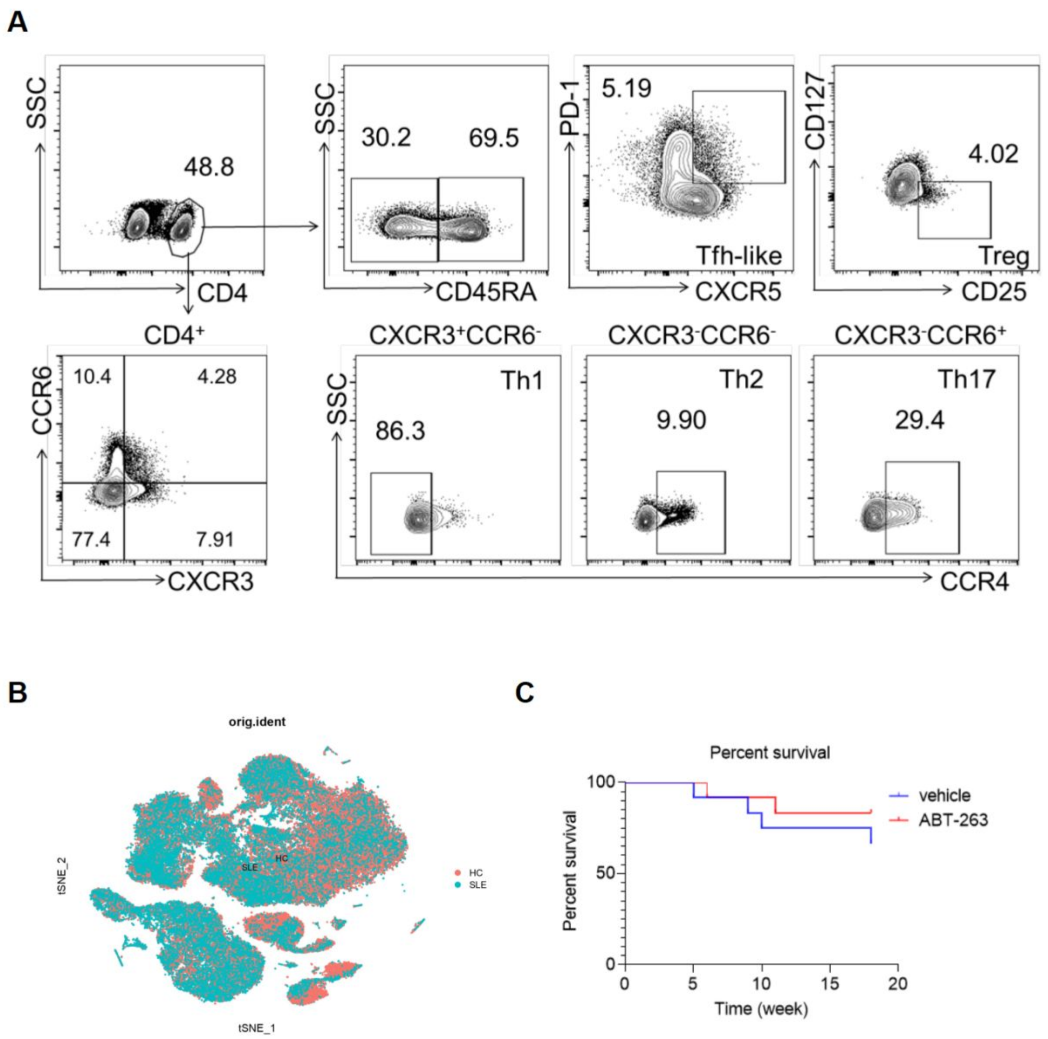

Figure S2.

A. Representative flow diagrams of CD4$^+$ T cell subsets (Tfh-like, Treg, Th1, Th2, and Th17 cells) from CD4$^+$ T cell. **B.** The single-cell dataset of PBMCs from peripheral blood of SLE patients (n = 7) and HCs (n = 5) and perform dimensionality reduction with T-SNE revealing 21 cell clusters. **C.** The survival curve of MRL/lpr mice treated with ABT-263 or vehicle.

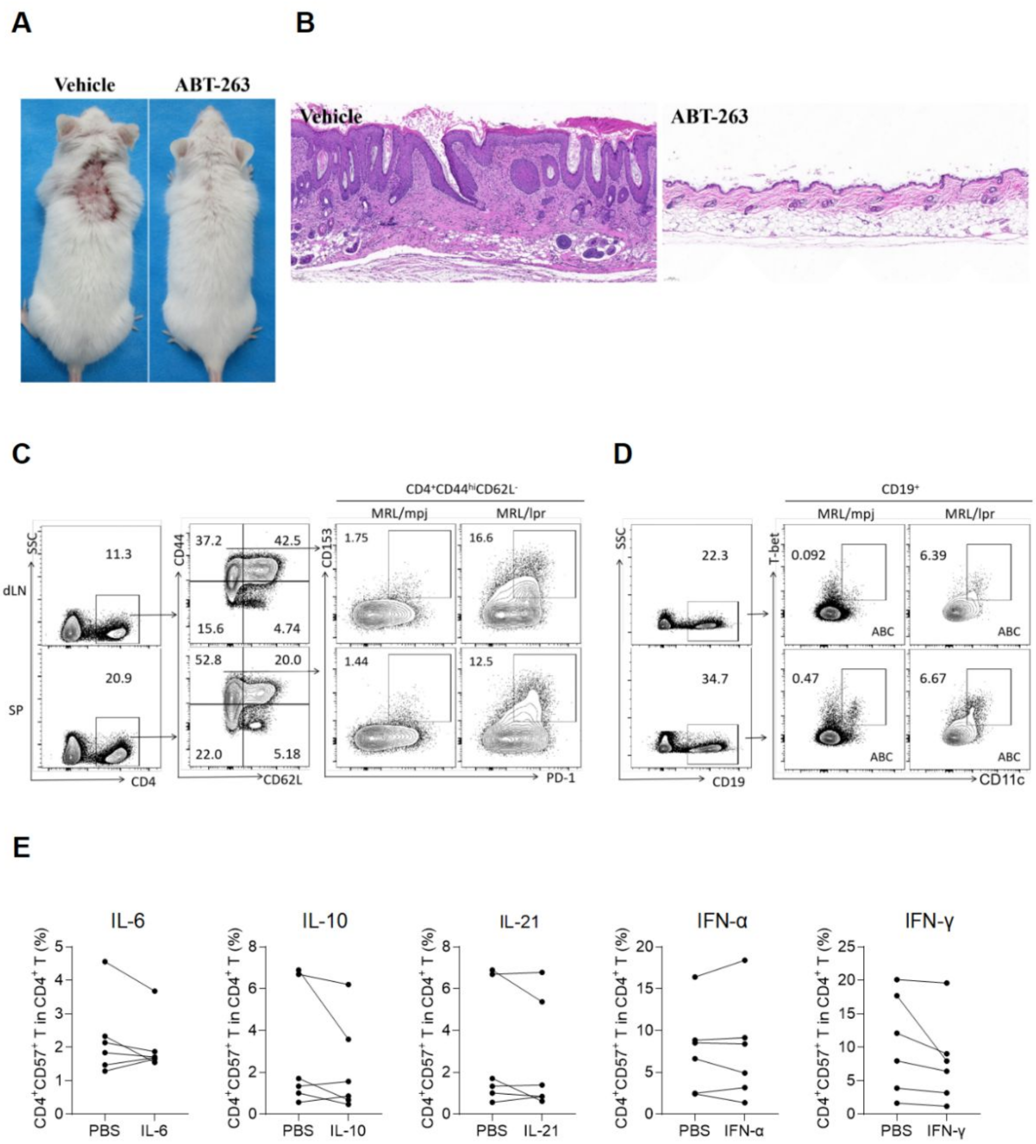

Figure S3.

A-B. Representative skin manifestations and H&E staining (× 200) of skin lesions of MRL/lpr mice treated with ABT-263 or vehicle. **C-D**. Representative flow diagrams of the frequency of senescent $CD4^+$ T cells ($CD4^+CD44^{hi}CD62L^-PD\text{-}1^+CD153^+$) and ABC ($CD19^+CD11c^+T\text{-}bet^+$) from the spleen and dLNs of MRL/lpr (n = 3) and MRL/mpj mice (n = 3). **E.** Statistical analysis of the frequency of senescent $CD4^+$ T cells in $CD4^+$ T cells from PBMC stimulated with 20 ng/mL IL-6 (n = 6), IL-10 (n =

6), IL-21 (n = 6), IFN-α (n = 6), IFN-γ (n = 6) or PBS (n = 6).

Table S1A. Detailed information of samples for flow cytometry

No.	Gender	Age (year)	SLEDAI Score	No.	Gender	Age (year)
SLE1	F	33	2	RA1	F	54
SLE2	F	27	2	RA2	F	63
SLE3	F	57	1	RA3	F	37
SLE4	F	37	9	RA4	F	67
SLE5	F	58	2	RA5	M	56
SLE6	F	43	4	RA6	F	45
SLE7	F	31	4	RA7	F	52
SLE8	F	35	4	RA8	M	69
SLE9	F	52	4	RA9	F	52
SLE10	F	24	2	RA10	F	43
SLE11	F	22	3	HC1	F	54
SLE12	F	39	3	HC2	F	52
SLE13	F	53	6	HC3	F	43
SLE14	F	21	4	HC4	F	32
SLE15	F	49	10	HC5	F	36
SLE16	M	52	3	HC6	F	31
SLE17	F	35	2	HC7	F	38
SLE18	M	55	2	HC8	F	40

SLE19	F	15	0	HC9	F	44
SLE20	M	35	6	HC10	F	31
SLE21	F	44	2	HC11	F	40
SLE22	F	16	4			
SLE23	F	15	0			
SLE24	F	16	17			
SLE25	F	28	10			
SLE26	F	27	7			
SLE27	F	27	1			
SLE28	F	18	0			
SLE29	F	19	1			

Abbreviation: SLE, Systemic Lupus Erythematosus; RA, Rheumatoid Arthritis; HC, Health Control; F, Female; M, Male.

Table S1B. Detailed information of samples for flow cytometry

No.	Gender	Age (year)	No.	Gender	Age (year)
SLE1	F	20	RA1	F	33
SLE2	F	33	RA2	F	51
SLE3	F	19	RA3	F	40
SLE4	M	24	RA4	F	48
SLE5	F	34	RA5	F	44
SLE6	F	50	RA6	F	42
SLE7	M	66	RA7	F	50
SLE8	F	23	RA8	F	54
SLE9	F	21	HC1	F	19
SLE10	F	18	HC2	F	23
SLE11	F	34	HC3	F	46
SLE12	M	35	HC4	F	42
SLE13	F	48	HC5	F	38
SLE14	F	20	HC6	F	38
SLE15	F	29	HC7	F	27
SLE16	F	42	HC8	F	43
SLE17	M	34	HC9	F	26
SLE18	M	44	HC10	M	27
SLE19	M	50			

SLE20	F	32

Abbreviation: SLE, Systemic Lupus Erythematosus; RA, Rheumatoid Arthritis; HC, Health Control; F, Female.

Table S1C. Detailed information of samples for flow cytometry

No.	Gender	Age (year)	No.	Gender	Age (year)
SLE1	F	39	SLE17	M	21
SLE2	M	36	SLE18	F	33
SLE3	F	33	SLE19	F	39
SLE4	F	32	SLE20	F	34
SLE5	F	49	HC1	M	29
SLE6	F	33	HC2	F	42
SLE7	F	35	HC3	M	23
SLE8	F	34	HC4	F	44
SLE9	M	30	HC5	F	33
SLE10	F	26	HC6	M	36
SLE11	F	25	HC7	M	28
SLE12	F	37	HC8	F	33
SLE13	F	31	HC9	F	28
SLE14	F	46	HC10	F	38
SLE15	F	33	HC11	F	32
SLE16	F	27			

Abbreviation: SLE, Systemic Lupus Erythematosus; HC, Health Control; F, Female.

Table S1D. Detailed information of samples for RT-qPCR

No.	Gender	Age (year)	SLEDAI Score	No.	Gender	Age (year)
SLE1	F	28	12	HC1	F	40
SLE2	F	47	10	HC2	F	49
SLE3	F	30	5	HC3	F	32
SLE4	F	66	8	HC4	F	36
SLE5	F	57	4	HC5	F	28
SLE6	F	39	10	HC6	F	34
SLE7	F	34	NA	HC7	F	35
SLE8	F	41	2	HC8	F	28
SLE9	F	43	6	HC9	F	26
SLE10	F	52	4	HC10	F	33
SLE11	F	47	2	HC11	F	38
SLE12	F	25	4	HC12	F	42
SLE13	F	24	6	HC13	M	50
SLE14	F	16	10	HC14	F	47
SLE15	F	32	NA	HC15	F	38
SLE16	F	18	12	HC16	M	27
SLE17	F	24	8	HC17	F	29
SLE18	F	45	2	HC18	F	30
SLE19	F	57	22			

SLE20	F	28	8
SLE21	F	17	13
SLE22	F	30	4
SLE23	F	30	0
SLE24	F	50	8
SLE25	F	34	16
SLE26	M	23	4
SLE27	F	17	6
SLE28	F	NA	0
SLE29	F	19	16
SLE30	F	22	12
SLE31	F	29	7
SLE32	F	32	6
SLE33	F	34	18
SLE34	F	17	0
SLE35	F	40	9
SLE36	F	14	7
SLE37	M	53	4
SLE38	M	30	16
SLE39	M	62	6

Abbreviation: SLE, Systemic Lupus Erythematosus; HC, Health Control; F, Female; M, Male; NA, Not Available.

Table S1E. Detailed information of healthy volunteers

No.	Gender	Age (year)	No.	Gender	Age (year)
1	F	26	18	F	29
2	M	33	19	F	46
3	M	33	20	F	34
4	F	49	21	F	45
5	F	40	22	F	32
6	F	46	23	F	28
7	M	25	24	F	29
8	F	39	25	F	30
9	F	38	26	F	26
10	F	39	27	F	29
11	F	29	28	F	31
12	F	24	29	M	25
13	M	41	30	F	22
14	M	39	31	F	24
15	F	25	32	F	21
16	F	39	33	M	30
17	F	33	34	F	23

Abbreviation: F, Female; M, Male.

Table S2. Detailed information of antibodies for flow cytometry.

Antibody	Application	Cat	Source
BD Pharmingen™ PerCP-Cy™5.5 Mouse Anti-Human CD4	Human	552838	BD
PE/Cyanine7 anti-human CD57 Antibody	Human	359624	Biolegend
BD Pharmingen™ FITC Mouse Anti-Human CD27	Human	555440	BD
PE anti-human CD28 Antibody	Human	302940	Biolegend
APC/Cyanine7 anti-human CD185 (CXCR5) Antibody	Human	356926	Biolegend
CD279 (PD-1) Monoclonal Antibody (eBioJ105 (J105)), APC, eBioscience™	Human	17-2799-42	eBioscience
CD4 Monoclonal Antibody (SK3 (SK-3)), FITC, eBioscience™	Human	11-0047-42	eBioscience
Brilliant Violet 711™ anti-human CD25 Antibody	Human	356138	Biolegend
PerCP/Cyanine5.5 anti-human CD127 (IL-7Rα) Antibody	Human	351322	Biolegend
Brilliant Violet 421™ anti-human CD183 (CXCR3) Antibody	Human	353716	Biolegend
Brilliant Violet 605™ anti-human CD194 (CCR4) Antibody	Human	359418	Biolegend
PE/Dazzle™ 594 anti-human CD196 (CCR6) Antibody	Human	353430	Biolegend
Brilliant Violet 785™ anti-human CD45RA Antibody	Human	304140	Biolegend
BD Pharmingen™ APC-Cy™7 Mouse Anti-Human CD4	Human	557871	BD
Alexa Fluor® 647 anti-Bcl-2 Antibody	Human	658705	Biolegend
BD Pharmingen™ FITC Rat Anti-Mouse CD4	Mouse	553729	BD
APC/Cyanine7 anti-mouse/human CD44 Antibody	Mouse	103028	Biolegend
PE/Cyanine7 anti-mouse CD62L Antibody	Mouse	104418	Biolegend

BD Pharmingen™ APC Hamster Anti-Mouse CD279 (PD-1)	Mouse	562671	BD
PE anti-mouse CD153 Antibody	Mouse	106405	Biolegend
PE/Cyanine7 anti-T-bet Antibody	Mouse	644824	Biolegend
BD Pharmingen™ APC Rat Anti-Mouse CD19	Mouse	550992	BD
PerCP/Cyanine5.5 anti-mouse CD11c Antibody	Mouse	117328	Biolegend
Brilliant Violet 605™ anti-mouse CD4 Antibody	Mouse	100451	Biolegend
PE-Cy7 anti-mouse CD44	Mouse	103030	Biolegend
Percp-Cy5.5 anti-mouse CD62L	Mouse	104432	Biolegend
Brilliant Violet 711™ anti-mouse CD19 Antibody	Mouse	115555	Biolegend
BD Pharmingen™ FITC Rat Anti-Mouse CD4	Mouse	553729	BD
PE anti-mouse CD25 Antibody	Mouse	102008	Biolegend
Anti-Mouse/Rat Foxp3 Staining Set APC, eBioscience™	Mouse	77-5775-40	eBioscience
BD Pharmingen™ Biotin Rat Anti-Mouse CD185 (CXCR5)	Mouse	551960	BD
BD Pharmingen™ PE Streptavidin	Mouse	554061	BD
BD Pharmingen™ APC Hamster Anti-Mouse CD279 (PD-1)	Mouse	562671	BD
PerCP/Cyanine5.5 anti-mouse/human CD45R/B220 Antibody	Mouse	103236	Biolegend
BD Pharmingen™ PE Hamster Anti-Mouse CD95	Mouse	554258	BD
BD Pharmingen™ Alexa Fluor® 647 Rat Anti-Mouse T- and B-Cell Activation Antigen	Mouse	561529	BD
Zombie NIR™ Fixable Viability Kit	Human/Mouse	423106	Biolegend
Zombie Aqua™ Fixable Viability Kit	Human/Mouse	423102	Biolegend

Table S3. The sequence of primers for RT-qPCR

Species	Genes	Primers	Sequences (5'-3')
Human	*CD57*	Forward Primer	CTCCTTCGAGAACTTGTCACC
		Reverse Primer	GGGTCAGTGAAGCCCTTCTT
Human	*p16*	Forward Primer	CTCCGGAAGCTGTCGACTTC
		Reverse Primer	TTCTGCCATTTGCTAGCAGTGT
Human	*P21*	Forward Primer	GAAGTGAGCACAGCCTAG
		Reverse Primer	TGCCTTCACAAGACAGAG
Human	*P53*	Forward Primer	GCGTGTGGAGTATTTGGATGAC
		Reverse Primer	ATGTAGTTGTAGTGGATGGTGGTA
Human	*IL6*	Forward Primer	ACTCACCTCTTCAGAACGAATTG
		Reverse Primer	CCATCTTTGGAAGGTTCAGGTTG
Human	*IL8*	Forward Primer	ACTGAGAGTGATTGAGAGTGGAC
		Reverse Primer	AACCCTCTGCACCCAGTTTTC
Human	*TNFα*	Forward Primer	CCTCTCTCTAATCAGCCCTCTG
		Reverse Primer	GAGGACCTGGGAGTAGATGAG
Human	*BCL2*	Forward Primer	GAGCGTCAACAGGGAGATG
		Reverse Primer	CAGAGACAGCCAGGAGAAATC
Human	*BCLxL*	Forward Primer	GGAAAGCGTAGACAAGGAGATG
		Reverse Primer	CCCGTAGAGATCCACAAAAGTG
Human	*IL1β*	Forward Primer	TTCGACACATGGGATAACGAGG

Species	Genes	Primers	Sequences (5'-3')
		Reverse Primer	TTTTTGCTGTGAGTCCCGGAG
Human	IL15	Forward Primer	AACAGAAGCCAACTGGGTGAATG
		Reverse Primer	CTCCAAGAGAAAGCACTTCATTGC
Human	IL15R	Forward Primer	TGGCTATCTCCACGTCCACTGT
		Reverse Primer	CATGGCTTCCATTTCAACGCTGG
Human	*EIF2AK2*	Forward Primer	ACGCTTTGGGGCTAATTCTTG
		Reverse Primer	CCCGTAGGTCTGTGAAAAACTT
Human	*UBE2I6*	Forward Primer	TGGACGAGAACGGACAGATTT
		Reverse Primer	GGCTCCCTGATATTCGGTCTATT
Human	*PSMB9*	Forward Primer	GGTTCTGATTCCCGAGTGTCT
		Reverse Primer	CAGCCAAAACAAGTGGAGGTT
Human	*BST2*	Forward Primer	CACACTGTGATGGCCCTAATG
		Reverse Primer	GTCCGCGATTCTCACGCTT
Human	*LY6E*	Forward Primer	CAGCTCGCTGATGTGCTTCT
		Reverse Primer	CAGACACAGTCACGCAGTAGT
Human	*RGS1*	Forward Primer	TCTTCTCTGCTAACCCAAAGGA
		Reverse Primer	TGCTTTACAGGGCAAAAGATCAG
Human	*NT5C3A*	Forward Primer	TCACATGGTTTGCTTGTTCAGC
		Reverse Primer	AGCATAACGTCAGATTCTGCC
Human	*Sp100*	Forward Primer	TCCCCATCTCATGCTGGTACA
		Reverse Primer	TGGCTTCCTAGCGAATCATCTT

Species	Genes	Primers	Sequences (5'-3')
Human	*PSME2*	Forward Primer	TTTGGGGTAGCAATCCAGGAG
		Reverse Primer	CCAAGGCCCGGTAATCCAT
Human	*IFITM1*	Forward Primer	CCAAGGTCCACCGTGATTAAC
		Reverse Primer	ACCAGTTCAAGAAGAGGGTGTT
Human	*GADPH*	Forward Primer	GGAGCGAGATCCCTCCAAAAT
		Reverse Primer	GGCTGTTGTCATACTTCTCATGG
Mouse	*p16*	Forward Primer	GAACTCTTTCGGTCGTACCC
		Reverse Primer	AGTTCGAATCTGCACCGTAGT
Mouse	*p21*	Forward Primer	GAACATCTCAGGGCCGAAAA
		Reverse Primer	TGCGCTTGGAGTGATAGAAATC
Mouse	*p53*	Forward Primer	TCACAGCGTCTGTTGACATTT
		Reverse Primer	ACCAAGCTCATTACCCTGACA
Mouse	*Il1β*	Forward Primer	GCAACTGTTCCTGAACTCAACT
		Reverse Primer	ATCTTTTGGGGTCCGTCAACT
Mouse	*Il6*	Forward Primer	TAGTCCTTCCTACCCCAATTTCC
		Reverse Primer	TTGGTCCTTAGCCACTCCTTC
Mouse	*Mmp13*	Forward Primer	CTTCTTCTTGTTGAGCTGGACTC
		Reverse Primer	CTGTGGAGGTCACTGTAGACT
Mouse	*Bcl2*	Forward Primer	GAGCGTCAACAGGGAGATG
		Reverse Primer	CAGAGACAGCCAGGAGAAATC
Mouse	*Bclxl*	Forward Primer	GGAAAGCGTAGACAAGGAGATG

Species	Genes	Primers	Sequences (5'-3')
		Reverse Primer	CCCGTAGAGATCCACAAAAGTG
Mouse	*Stat1*	Forward Primer	GCTGCCTATGATGTCTCGTTT
		Reverse Primer	TGCTTTTCCGTATGTTGTGCT
Mouse	*Stat3*	Forward Primer	CAATACCATTGACCTGCCGAT
		Reverse Primer	GAGCGACTCAAACTGCCCT
Mouse	*Ube2l6*	Forward Primer	GACGATGCCAATGTGCTTGTG
		Reverse Primer	CTGGGGAAATCAATCCGCACT
Mouse	*Bst2*	Forward Primer	TGTTCGGGGTTACCTTAGTCA
		Reverse Primer	GCAGGAGTTTGCCTGTGTCT
Mouse	*Rgs1*	Forward Primer	TCTGGGATGAAATCGGCCAAG
		Reverse Primer	GCATCTGAATGCACAAATGCTT
Mouse	*Sp100*	Forward Primer	AGCTACAACCACAGTCCCCT
		Reverse Primer	TCCTGTCCTTTTCCGTCTTCTAA
Mouse	*β-actin*	Forward Primer	GCTCTTTTCCAGCCTTCCTT
		Reverse Primer	CTTCTGCATCCTGTCAGCAA

Supplemental file

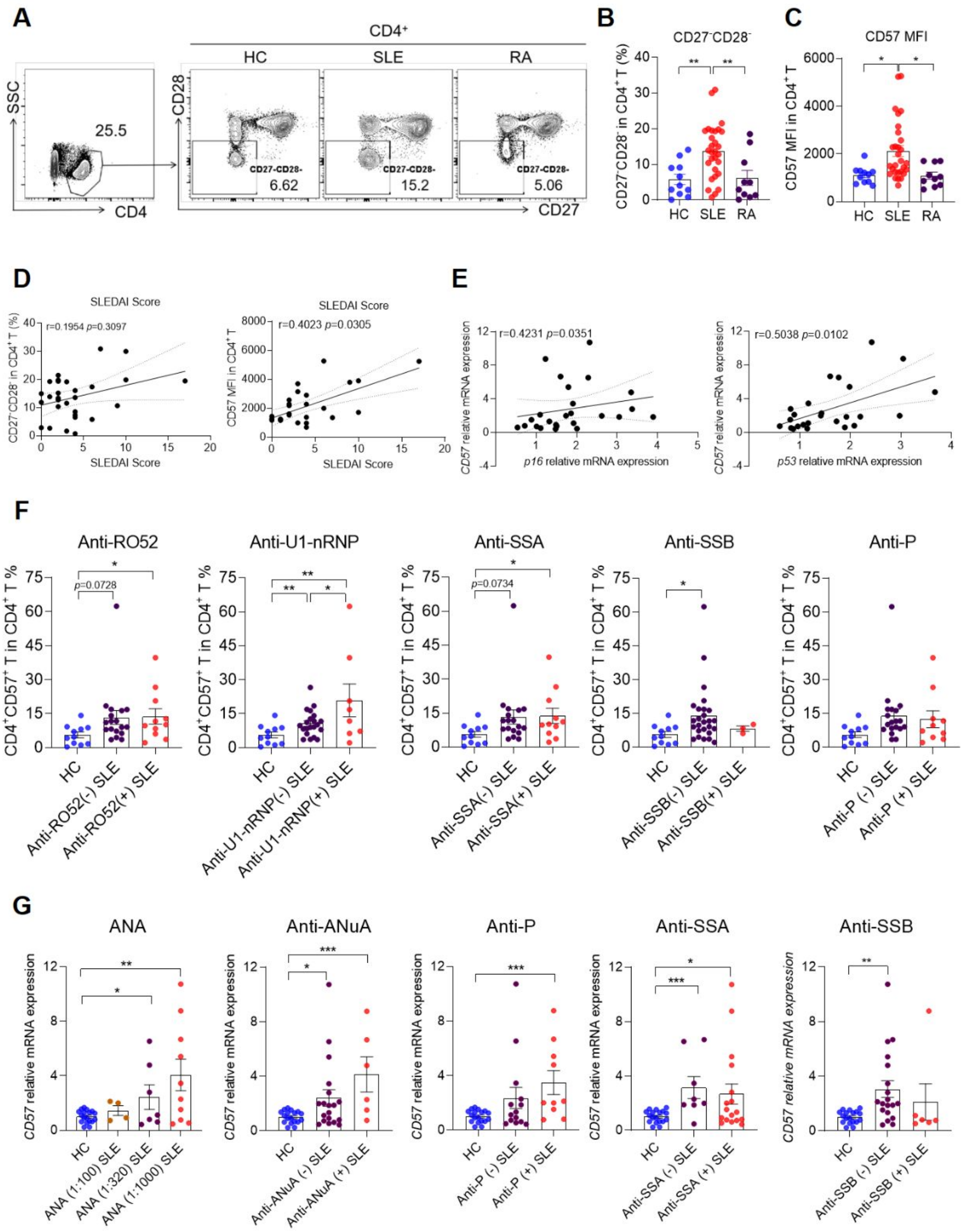

Figure S1.

A-B. Representative flow diagrams of gating and statistical analysis for $CD4^{+}CD27^{-}CD28^{-}$ T cells in $CD4^{+}$ T cells from peripheral blood of SLE patients (n = 29), RA patients (n = 10), and HCs (n = 11). **C.** Statistical analysis of the MFI of CD57 in $CD4^{+}$ T cells from peripheral blood of SLE patients (n = 29), RA patients (n = 10), and HCs (n = 11). **D**. Correlation of the frequency of $CD27^{-}CD28^{-}$ cells and the MFI of CD57 in $CD4^{+}$ T cells with the SLEDAI score in SLE patients (n = 29). **E.** Correlation of the mRNA expression levels of p16 and p53 in $CD4^{+}$ T cells with the mRNA expression levels of CD57 in SLE patients (n = 29). **F-G**. Statistical analysis of the proportion of senescent $CD4^{+}$ T cells and the mRNA expression levels of CD57 of the $CD4^{+}$ T cells in distinct SLE patient groups and HCs. Horizontal bars represent the mean ± SEM. * $p < 0.05$, ** $p < 0.01$, *** $p < 0.001$, and r = spearman rank sum correlation coefficient.

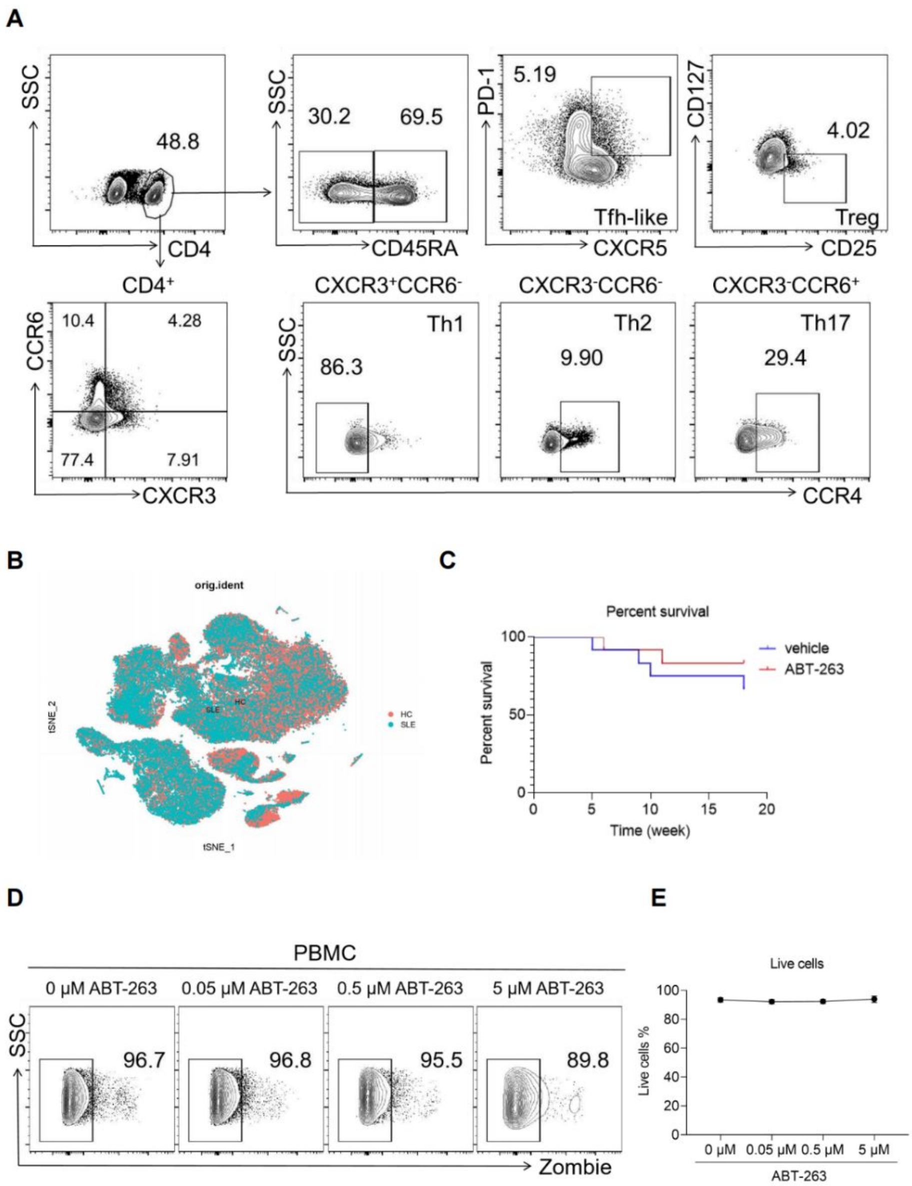
A
SSC
48.8
CD4
30.2
69.5
CD45RA
PD-1
5.19
Tfh-like
CXCR5
CD127
4.02
Treg
CD25
CD4⁺
CCR6
10.4
4.28
77.4
7.91
CXCR3
CXCR3⁺CCR6⁻
CXCR3⁻CCR6⁻
CXCR3⁻CCR6⁺
Th1
86.3
Th2
9.90
Th17
29.4
CCR4
B
orig.ident
tSNE_2
tSNE_1
HC
SLE
C
Percent survival
vehicle
ABT-263
Percent survival
Time (week)
D
PBMC
0 μM ABT-263
0.05 μM ABT-263
0.5 μM ABT-263
5 μM ABT-263
96.7
96.8
95.5
89.8
Zombie
E
Live cells
Live cells %
0 μM
0.05 μM
0.5 μM
5 μM
ABT-263

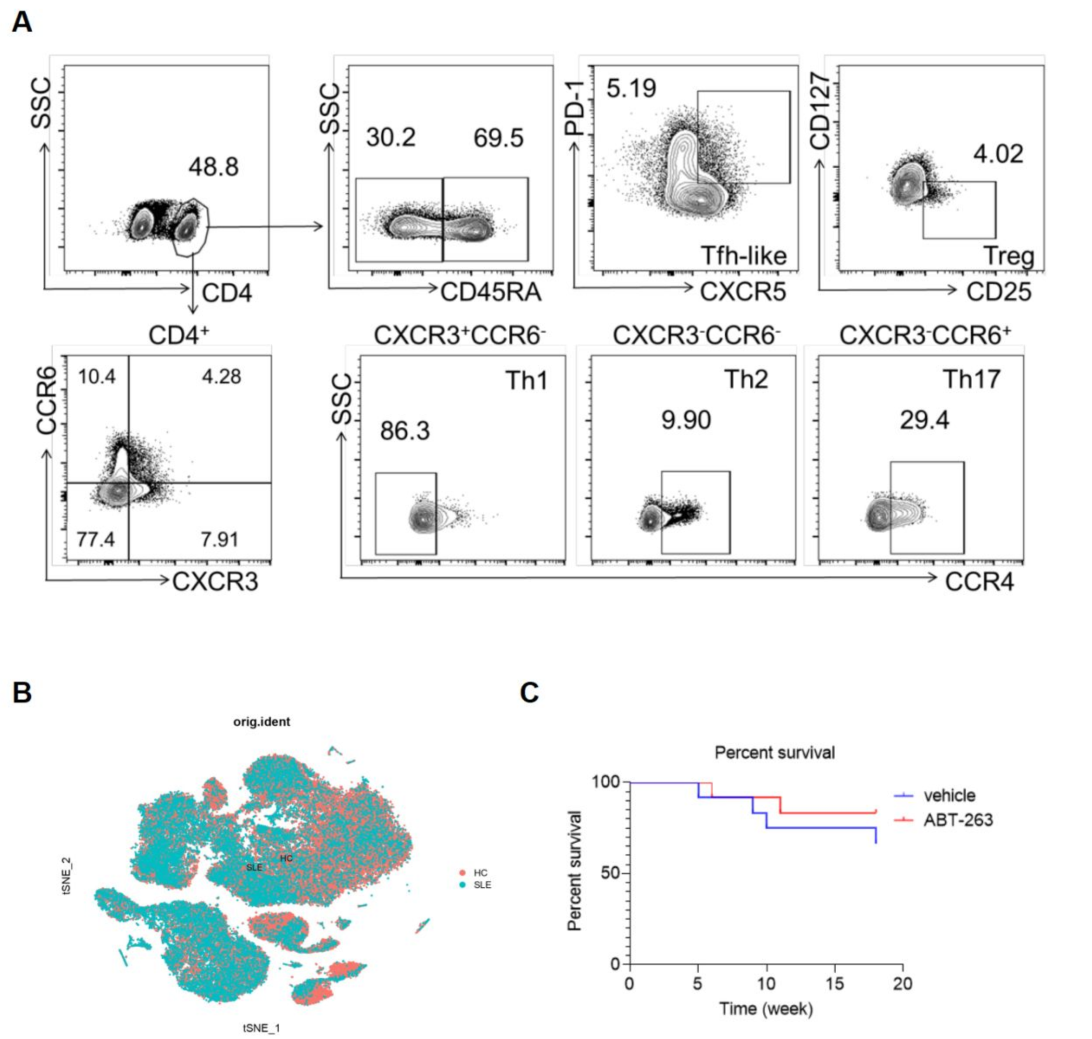

Figure S2.

A. Representative flow diagrams of CD4+ T cell subsets (Tfh-like, Treg, Th1, Th2, and Th17 cells) from CD4+ T cell. **B.** The single-cell dataset of PBMCs from peripheral blood of SLE patients (n = 7) and HCs (n = 5) and perform dimensionality reduction with T-SNE revealing 21 cell clusters. **C.** The survival curve of MRL/lpr mice treated with ABT-263 or vehicle. ~~**D-E.** Representative flow diagrams and statistical analysis of the frequency of live cells from lymphocytes of PBMC stimulated with 0 (n = 6), 0.05 (n = 6), 0.5 (n = 6), and 5 μM (n = 6) respectively for~~

~~72 hours.~~

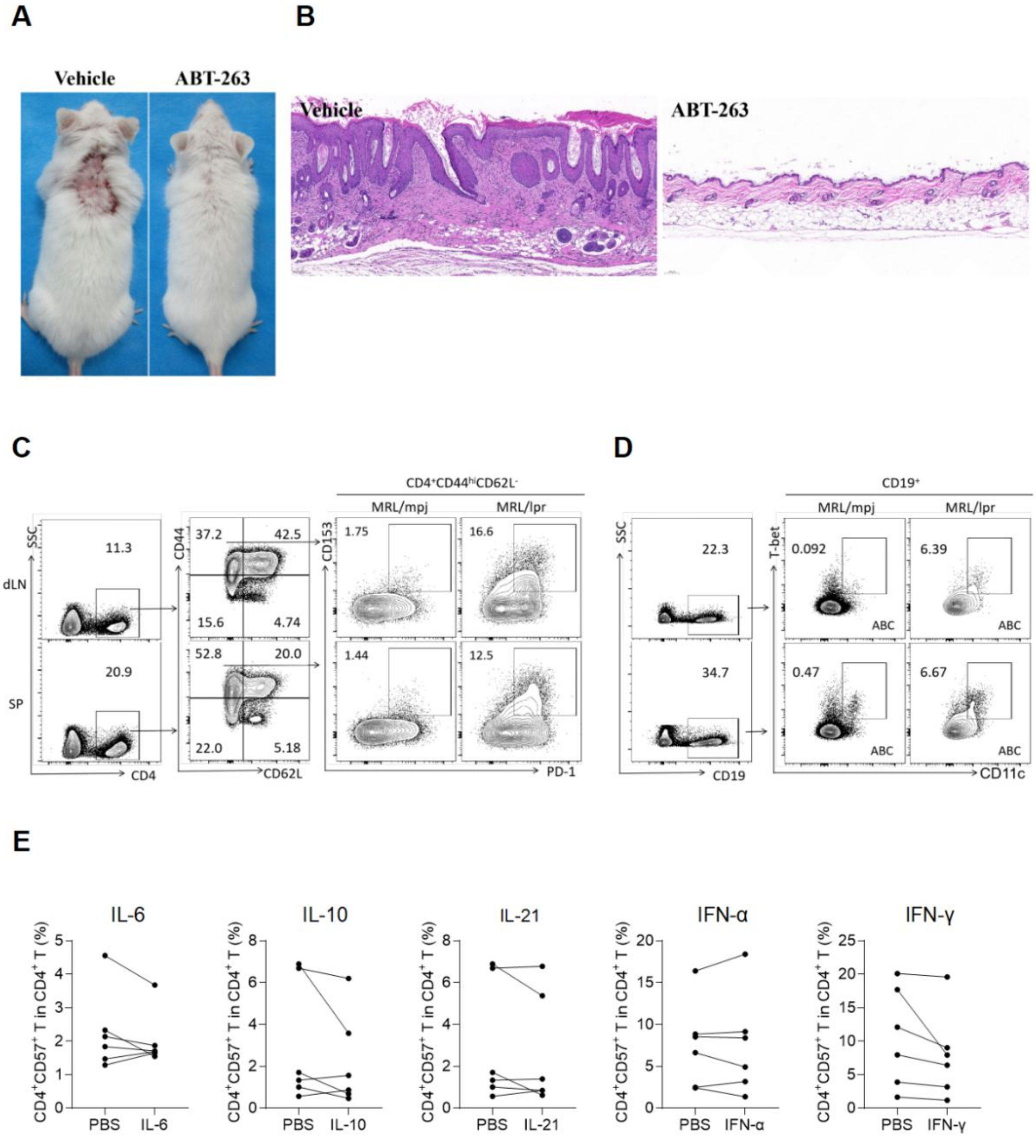

Figure S3.

A-B. Representative skin manifestations and H&E staining (× 200) of skin lesions of MRL/lpr mice treated with ABT-263 or vehicle. **C-D**. Representative flow diagrams of the frequency of senescent $CD4^+$ T cells ($CD4^+CD44^{hi}CD62L^-PD\text{-}1^+CD153^+$) and ABC ($CD19^+CD11c^+T\text{-}bet^+$) from the spleen and dLNs of MRL/lpr (n = 3) and

MRL/mpj mice (n = 3). **E.** Statistical analysis of the frequency of senescent CD4$^+$ T cells in CD4$^+$ T cells from PBMC stimulated with 20 ng/mL IL-6 (n = 6), IL-10 (n = 6), IL-21 (n = 6), IFN-α (n = 6), IFN-γ (n = 6) or PBS (n = 6).

Table S1A. Detailed information of samples for flow cytometry

No.	Gender	Age (year)	SLEDAI Score	No.	Gender	Age (year)
SLE1	F	33	2	RA1	F	54
SLE2	F	27	2	RA2	F	63
SLE3	F	57	1	RA3	F	37
SLE4	F	37	9	RA4	F	67
SLE5	F	58	2	RA5	M	56
SLE6	F	43	4	RA6	F	45
SLE7	F	31	4	RA7	F	52
SLE8	F	35	4	RA8	M	69
SLE9	F	52	4	RA9	F	52
SLE10	F	24	2	RA10	F	43
SLE11	F	22	3	HC1	F	54
SLE12	F	39	3	HC2	F	52
SLE13	F	53	6	HC3	F	43
SLE14	F	21	4	HC4	F	32
SLE15	F	49	10	HC5	F	36
SLE16	M	52	3	HC6	F	31

SLE17	F	35	2	HC7	F	38
SLE18	M	55	2	HC8	F	40
SLE19	F	15	0	HC9	F	44
SLE20	M	35	6	HC10	F	31
SLE21	F	44	2	HC11	F	40
SLE22	F	16	4			
SLE23	F	15	0			
SLE24	F	16	17			
SLE25	F	28	10			
SLE26	F	27	7			
SLE27	F	27	1			
SLE28	F	18	0			
SLE29	F	19	1			

Abbreviation: SLE, Systemic Lupus Erythematosus; RA, Rheumatoid Arthritis; HC, Health Control; F, Female; M, Male.

Table S1B. Detailed information of samples for flow cytometry

No.	Gender	Age (year)	No.	Gender	Age (year)
SLE1	F	20	RA1	F	33
SLE2	F	33	RA2	F	51
SLE3	F	19	RA3	F	40
SLE4	M	24	RA4	F	48
SLE5	F	34	RA5	F	44
SLE6	F	50	RA6	F	42
SLE7	M	66	RA7	F	50
SLE8	F	23	RA8	F	54
SLE9	F	21	HC1	F	19
SLE10	F	18	HC2	F	23
SLE11	F	34	HC3	F	46
SLE12	M	35	HC4	F	42
SLE13	F	48	HC5	F	38
SLE14	F	20	HC6	F	38
SLE15	F	29	HC7	F	27
SLE16	F	42	HC8	F	43
SLE17	M	34	HC9	F	26
SLE18	M	44	HC10	M	27
SLE19	M	50			

SLE20	F	32

Abbreviation: SLE, Systemic Lupus Erythematosus; RA, Rheumatoid Arthritis; HC, Health Control; F, Female.

Table S1C. Detailed information of samples for flow cytometry

No.	Gender	Age (year)	No.	Gender	Age (year)
SLE1	F	39	SLE17	M	21
SLE2	M	36	SLE18	F	33
SLE3	F	33	SLE19	F	39
SLE4	F	32	SLE20	F	34
SLE5	F	49	HC1	M	29
SLE6	F	33	HC2	F	42
SLE7	F	35	HC3	M	23
SLE8	F	34	HC4	F	44
SLE9	M	30	HC5	F	33
SLE10	F	26	HC6	M	36
SLE11	F	25	HC7	M	28
SLE12	F	37	HC8	F	33
SLE13	F	31	HC9	F	28
SLE14	F	46	HC10	F	38
SLE15	F	33	HC11	F	32
SLE16	F	27			

Abbreviation: SLE, Systemic Lupus Erythematosus; HC, Health Control; F, Female.

Table S1D. Detailed information of samples for RT-qPCR

No.	Gender	Age (year)	SLEDAI Score	No.	Gender	Age (year)
SLE1	F	28	12	HC1	F	40
SLE2	F	47	10	HC2	F	49
SLE3	F	30	5	HC3	F	32
SLE4	F	66	8	HC4	F	36
SLE5	F	57	4	HC5	F	28
SLE6	F	39	10	HC6	F	34
SLE7	F	34	NA	HC7	F	35
SLE8	F	41	2	HC8	F	28
SLE9	F	43	6	HC9	F	26
SLE10	F	52	4	HC10	F	33
SLE11	F	47	2	HC11	F	38
SLE12	F	25	4	HC12	F	42
SLE13	F	24	6	HC13	M	50
SLE14	F	16	10	HC14	F	47
SLE15	F	32	NA	HC15	F	38
SLE16	F	18	12	HC16	M	27
SLE17	F	24	8	HC17	F	29
SLE18	F	45	2	HC18	F	30
SLE19	F	57	22			

SLE20	F	28	8
SLE21	F	17	13
SLE22	F	30	4
SLE23	F	30	0
SLE24	F	50	8
SLE25	F	34	16
SLE26	M	23	4
SLE27	F	17	6
SLE28	F	NA	0
SLE29	F	19	16
SLE30	F	22	12
SLE31	F	29	7
SLE32	F	32	6
SLE33	F	34	18
SLE34	F	17	0
SLE35	F	40	9
SLE36	F	14	7
SLE37	M	53	4
SLE38	M	30	16
SLE39	M	62	6

Abbreviation: SLE, Systemic Lupus Erythematosus; HC, Health Control; F, Female; M, Male; NA, Not Available.

Table S1E. Detailed information of healthy volunteers

No.	Gender	Age (year)	No.	Gender	Age (year)
1	F	26	18	F	29
2	M	33	19	F	46
3	M	33	20	F	34
4	F	49	21	F	45
5	F	40	22	F	32
6	F	46	23	F	28
7	M	25	24	F	29
8	F	39	25	F	30
9	F	38	26	F	26
10	F	39	27	F	29
11	F	29	28	F	31
12	F	24	29	M	25
13	M	41	30	F	22
14	M	39	31	F	24
15	F	25	32	F	21
16	F	39	33	M	30
17	F	33	34	F	23

Abbreviation: F, Female; M, Male.

Table S2. Detailed information of antibodies for flow cytometry.

Antibody	Application	Cat	Source
BD Pharmingen™ PerCP-Cy™5.5 Mouse Anti-Human CD4	Human	552838	BD
PE/Cyanine7 anti-human CD57 Antibody	Human	359624	Biolegend
BD Pharmingen™ FITC Mouse Anti-Human CD27	Human	555440	BD
PE anti-human CD28 Antibody	Human	302940	Biolegend
APC/Cyanine7 anti-human CD185 (CXCR5) Antibody	Human	356926	Biolegend
CD279 (PD-1) Monoclonal Antibody (eBioJ105 (J105)), APC, eBioscience™	Human	17-2799-42	eBioscience
CD4 Monoclonal Antibody (SK3 (SK-3)), FITC, eBioscience™	Human	11-0047-42	eBioscience
Brilliant Violet 711™ anti-human CD25 Antibody	Human	356138	Biolegend
PerCP/Cyanine5.5 anti-human CD127 (IL-7Rα) Antibody	Human	351322	Biolegend
Brilliant Violet 421™ anti-human CD183 (CXCR3) Antibody	Human	353716	Biolegend
Brilliant Violet 605™ anti-human CD194 (CCR4) Antibody	Human	359418	Biolegend
PE/Dazzle™ 594 anti-human CD196 (CCR6) Antibody	Human	353430	Biolegend
Brilliant Violet 785™ anti-human CD45RA Antibody	Human	304140	Biolegend
BD Pharmingen™ APC-Cy™7 Mouse Anti-Human CD4	Human	557871	BD
Alexa Fluor® 647 anti-Bcl-2 Antibody	Human	658705	Biolegend
BD Pharmingen™ FITC Rat Anti-Mouse CD4	Mouse	553729	BD
APC/Cyanine7 anti-mouse/human CD44 Antibody	Mouse	103028	Biolegend
PE/Cyanine7 anti-mouse CD62L Antibody	Mouse	104418	Biolegend

BD Pharmingen™ APC Hamster Anti-Mouse CD279 (PD-1)	Mouse	562671	BD
PE anti-mouse CD153 Antibody	Mouse	106405	Biolegend
PE/Cyanine7 anti-T-bet Antibody	Mouse	644824	Biolegend
BD Pharmingen™ APC Rat Anti-Mouse CD19	Mouse	550992	BD
PerCP/Cyanine5.5 anti-mouse CD11c Antibody	Mouse	117328	Biolegend
Brilliant Violet 605™ anti-mouse CD4 Antibody	Mouse	100451	Biolegend
PE-Cy7 anti-mouse CD44	Mouse	103030	Biolegend
Percp-Cy5.5 anti-mouse CD62L	Mouse	104432	Biolegend
Brilliant Violet 711™ anti-mouse CD19 Antibody	Mouse	115555	Biolegend
BD Pharmingen™ FITC Rat Anti-Mouse CD4	Mouse	553729	BD
PE anti-mouse CD25 Antibody	Mouse	102008	Biolegend
Anti-Mouse/Rat Foxp3 Staining Set APC, eBioscience™	Mouse	77-5775-40	eBioscience
BD Pharmingen™ Biotin Rat Anti-Mouse CD185 (CXCR5)	Mouse	551960	BD
BD Pharmingen™ PE Streptavidin	Mouse	554061	BD
BD Pharmingen™ APC Hamster Anti-Mouse CD279 (PD-1)	Mouse	562671	BD
PerCP/Cyanine5.5 anti-mouse/human CD45R/B220 Antibody	Mouse	103236	Biolegend
BD Pharmingen™ PE Hamster Anti-Mouse CD95	Mouse	554258	BD
BD Pharmingen™ Alexa Fluor® 647 Rat Anti-Mouse T- and B-Cell Activation Antigen	Mouse	561529	BD
Zombie NIR™ Fixable Viability Kit	Human/Mouse	423106	Biolegend
Zombie Aqua™ Fixable Viability Kit	Human/Mouse	423102	Biolegend

Table S3. The sequence of primers for RT-qPCR

Species	Genes	Primers	Sequences (5'-3')
Human	*CD57*	Forward Primer	CTCCTTCGAGAACTTGTCACC
		Reverse Primer	GGGTCAGTGAAGCCCTTCTT
Human	*p16*	Forward Primer	CTCCGGAAGCTGTCGACTTC~~GGGTCAGTGAAGCCCTTCTT~~
		Reverse Primer	TTCTGCCATTTGCTAGCAGTGT
Human	*P21*	Forward Primer	GAAGTGAGCACAGCCTAG
		Reverse Primer	TGCCTTCACAAGACAGAG
Human	*P53*	Forward Primer	GCGTGTGGAGTATTTGGATGAC
		Reverse Primer	ATGTAGTTGTAGTGGATGGTGGTA
Human	*IL6*	Forward Primer	ACTCACCTCTTCAGAACGAATTG

Species	Genes	Primers	Sequences (5'-3')
		Reverse Primer	CCATCTTTGGAAGGTTCAGGTTG
Human	*IL8*	Forward Primer	ACTGAGAGTGATTGAGAGTGGAC
		Reverse Primer	AACCCTCTGCACCCAGTTTTC
Human	*TNFα*	Forward Primer	CCTCTCTCTAATCAGCCCTCTG
		Reverse Primer	GAGGACCTGGGAGTAGATGAG
Human	*BCL2*	Forward Primer	GAGCGTCAACAGGGAGATG
		Reverse Primer	CAGAGACAGCCAGGAGAAATC
Human	*BCLxL*	Forward Primer	GGAAAGCGTAGACAAGGAGATG
		Reverse Primer	CCCGTAGAGATCCACAAAAGTG
Human	*IL1β*	Forward Primer	TTCGACACATGGGATAACGAGG

Species	Genes	Primers	Sequences (5’-3’)
		Reverse Primer	TTTTTGCTGTGAGTCCCGGAG
Human	IL15	Forward Primer	AACAGAAGCCAACTGGGTGAATG
		Reverse Primer	CTCCAAGAGAAAGCACTTCATTGC
Human	IL15R	Forward Primer	TGGCTATCTCCACGTCCACTGT
		Reverse Primer	CATGGCTTCCATTTCAACGCTGG
Human	*EIF2AK2*	Forward Primer	ACGCTTTGGGGCTAATTCTTG
		Reverse Primer	CCCGTAGGTCTGTGAAAAACTT
Human	*UBE2I6*	Forward Primer	TGGACGAGAACGGACAGATTT
		Reverse Primer	GGCTCCCTGATATTCGGTCTATT
Human	*PSMB9*	Forward Primer	GGTTCTGATTCCCGAGTGTCT

Species	Genes	Primers	Sequences (5'-3')
Human	*BST2*	Reverse Primer	CAGCCAAAACAAGTGGAGGTT
		Forward Primer	CACACTGTGATGGCCCTAATG
Human	*LY6E*	Reverse Primer	GTCCGCGATTCTCACGCTT
		Forward Primer	CAGCTCGCTGATGTGCTTCT
Human	*RGS1*	Reverse Primer	CAGACACAGTCACGCAGTAGT
		Forward Primer	TCTTCTCTGCTAACCCAAAGGA
Human	*NT5C3A*	Reverse Primer	TGCTTTACAGGGCAAAAGATCAG
		Forward Primer	TCACATGGTTTGCTTGTTCAGC
Human	*Sp100*	Reverse Primer	AGCATAACGTCAGATTCTGCC
		Forward Primer	TCCCCATCTCATGCTGGTACA

Species	Genes	Primers	Sequences (5'-3')
Human	*PSME2*	Reverse Primer	TGGCTTCCTAGCGAATCATCTT
		Forward Primer	TTTGGGGTAGCAATCCAGGAG
Human	*IFITM1*	Reverse Primer	CCAAGGCCCGGTAATCCAT
		Forward Primer	CCAAGGTCCACCGTGATTAAC
Human	*GADPH*	Reverse Primer	ACCAGTTCAAGAAGAGGGTGTT
		Forward Primer	GGAGCGAGATCCCTCCAAAAT
		Reverse Primer	GGCTGTTGTCATACTTCTCATGG
Mouse	*p16*	Forward Primer	GAACTCTTTCGGTCGTACCC
		Reverse Primer	AGTTCGAATCTGCACCGTAGT
Mouse	*p21*	Forward Primer	GAACATCTCAGGGCCGAAAA

Species	**Genes**	**Primers**	**Sequences (5'-3')**
		Reverse Primer	TGCGCTTGGAGTGATAGAAATC
Mouse	*p53*	Forward Primer	TCACAGCGTCTGTTGACATTT
		Reverse Primer	ACCAAGCTCATTACCCTGACA
Mouse	*Il1β*	Forward Primer	GCAACTGTTCCTGAACTCAACT
		Reverse Primer	ATCTTTTGGGGTCCGTCAACT
Mouse	*Il6*	Forward Primer	TAGTCCTTCCTACCCCAATTTCC
		Reverse Primer	TTGGTCCTTAGCCACTCCTTC
Mouse	*Mmp13*	Forward Primer	CTTCTTCTTGTTGAGCTGGACTC
		Reverse Primer	CTGTGGAGGTCACTGTAGACT
Mouse	*Bcl2*	Forward Primer	GAGCGTCAACAGGGAGATG

Species	Genes	Primers	Sequences (5'-3')
		Reverse Primer	CAGAGACAGCCAGGAGAAATC
Mouse	*Bclxl*	Forward Primer	GGAAAGCGTAGACAAGGAGATG
		Reverse Primer	CCCGTAGAGATCCACAAAAGTG
Mouse	*Stat1*	Forward Primer	GCTGCCTATGATGTCTCGTTT
		Reverse Primer	TGCTTTTCCGTATGTTGTGCT
Mouse	*Stat3*	Forward Primer	CAATACCATTGACCTGCCGAT
		Reverse Primer	GAGCGACTCAAACTGCCCT
Mouse	*Ube2l6*	Forward Primer	GACGATGCCAATGTGCTTGTG
		Reverse Primer	CTGGGGAAATCAATCCGCACT
Mouse	*Bst2*	Forward Primer	TGTTCGGGGTTACCTTAGTCA

Species	**Genes**	**Primers**	**Sequences (5'-3')**
		Reverse Primer	GCAGGAGTTTGCCTGTGTCT
Mouse	*Rgs1*	Forward Primer	TCTGGGATGAAATCGGCCAAG
		Reverse Primer	GCATCTGAATGCACAAATGCTT
Mouse	*Sp100*	Forward Primer	AGCTACAACCACAGTCCCCT
		Reverse Primer	TCCTGTCCTTTTCCGTCTTCTAA
Mouse	*β-actin*	Forward Primer	GCTCTTTTCCAGCCTTCCTT
		Reverse Primer	CTTCTGCATCCTGTCAGCAA